Unsteady hydromagnetic chemically reacting mixed convection MHD flow over a permeable stretching sheet embedded in a porous medium with thermal radiation and heat source/sink

by

Machaba Mashudu Innocent

Supervisor: Prof Stanford Shateyi

Co-Supervisor: Ms. N.J. Netshiozwi

University of Venda

April 11, 2018

Abstract

The unsteady hydromagnetic chemically reacting mixed convection MHD flow over a permeable stretching sheet embedded in a porous medium with thermal radiation and heat source/sink is investigated numerically. The original partial differential equations are converted into ordinary differential equations by using similarity transformation. The governing non-linear partial differential equations of Momentum, Energy, and Concentration are considered in this study. The effects of various physical parameters on the velocity, temperature, and species concentration have been discussed. The parameters include the Prandtl number (Pr), Magnetic parameter (M), the Schmidt number (Sc), Unsteady parameter (A), buoyancy forces ratio parameter (N), Chemical reaction (K), Radiation parameter (Nr), Eckert number (Ec), local heat source/sink parameter (Q) and buoyancy parameter due to temperature (λ). The coefficient of Skin friction and Heat transfer are investigated. The coupled non-linear partial differential equations governing the flow field have been solved numerically using the Spectral Relaxation Method (SRM). The results that are obtained in this study are then presented in tabular forms and on graphs and the observations are discussed.

Keywords: Magnetohydrodynamics, Chemically reacting, Mixed convection, Stretching sheet, Porous medium, Thermal radiation and Heat source/sink.

DECLARATION

I hereby declare that this dissertation is my own original work and has not been submitted before to any institution for assessment purposes. Further, I have acknowledged all sources used and have cited these in the reference section.

Signature:..... Date:.....

ACKNOWLEDGEMENTS

Firstly, I would like to extend my earnest gratitude to my Supervisor Prof. Stanford Shateyi for the undying continuous support throughout my Master's research, for his patience, edification, enthusiasm, and vast knowledge. His guidance and assistance until the time for submission this thesis.

My thankfulness will not be complete if I forget the efforts of my Co-Supervisor Ms N.J Netshiozwi and my HOD Dr Simiso Moyo including my fellow students in Department of Mathematics and Applied Mathematics: Mrs Nancy Mukwevho and Ndou Ndivhuwo for the sleepless nights we were working together before the deadline and all the fun we had in the last two years.

My sincere thankfulness also goes to my family: my dearest mom, Ms Bernadette Machaba and my brothers, Khodani Machaba and Rotshidzwa Machaba for their support.

Contents

List of Tables

List of Figures

Index of Abbreviations

The following abbreviations are used in this study:

MHD	Magnetohydrodynamics
PDEs	Partial differential equations
ODEs	Ordinary differential equations
PST	Prescribed stretching surface temperature
PHF	Prescribed stretching surface heat flux
BVP	Boundary value problems
SRM	Spectral relaxation method

List of the main symbols

Variables and Parameters	Description
a	constant variable
A	unsteady parameter
b	constant variable
B_0	magnetic induction
C	concentration of species
C_f	local skin friction coefficient
c_p	Specific heat capacity
C_∞	Species concentration far from the surface
D	mass diffusivity
Ec	Eckert number
f	dimensionless stream function
G_r	Grashof number due to temperature
G_{r^*}	Grashof number due to concentration
K	chemical reaction
k^*	mean absorption coefficient
m	constant variable
M	magnetic parameter
N	buoyancy forces ratio parameter
Nr	radiation parameter
Nu_x	local Nusselt number
Pr	Prandtl number
Q	local heat source/sink parameter
q_r	radiative heat flux
s	local suction/injection parameter
Sc	Schmidt number
Sh_x	local Sherwood number

Variables and Parameters	Description
t	time
T	fluid temperature
T_w	wall temperature
T_∞	fluid temperature far away from the wall
u	velocity component in the x direction
U_w	stretching sheet wall velocity
v	velocity component in the y direction

Greek symbols

Variables and Parameters	Description
α	thermal diffusivity
α_∞	thermal diffusivity (m^2s^{-1})
β_C	volumetric coefficient of concentration expansion
β_T	volumetric coefficient of thermal expansion
η	transformed variable
θ	dimensionless temperature
λ	buoyancy parameter due to temperature
λ_1	The influence of buoyancy parameter on concentration
μ	dynamic viscosity $kgm^{-1}\ s^{-1}$
ν	kinematic viscosity (m^2s^{-1})
ρ	density of the fluid
σ	electrical conductivity of the fluid
σ^*	Stefan-Boltzmann constant
τ_w	wall shear stress
ϕ	dimensionless species concentration
ψ	stream function

Chapter 1

Introduction

This chapter gives a background introduction of the study followed by the statement of the problem which entails the main aim, objectives and hypothesis of the study. The chapter ends with a discussion of the definitions of keywords in the study.

1.1 Background of the study

This study deals with unsteady hydromagnetic chemically reacting mixed convection Magnetohydrodynamics (MHD) flow over a permeable stretching sheet embedded in a porous medium with thermal radiation and heat source/sink. The MHD is a dynamical system that can be governed by non-linear ordinary differential equations. The non-linear ordinary differential equation capture interacting processes during the magnetohydrodynamics. This system of equations is solved using either numerical methods or analytic methods such as perturbation ([32], [34]) to predict or portrait the behaviour of the system. In fluid dynamics, ordinary differential equations are utilised to elucidate the phenomenological mechanism governing the behaviour of a system. It is interesting to note that, in this study the Hydromagnetic chemically reaction is defined as the study of magnetic properties of electrically conducting fluids. The problems of hydromagnetic convective flow in a porous medium have attracted considerable attention in various scientific and technological applications. These various scientific and technological disciplines including but not limited to boundary layer flow control problems, plasma studies,

geothermal energy extraction, metallurgy, chemical, mineral and petroleum engineering, among others. The study of a flow over a stretching sheet began in the work of Crane [9], where the study reported that the unsteady boundary layer flow past a stretching plate and heat transfer with a variable thermal conductivity and further attempted the heat flow problems in prescribed stretching surface temperature (PST) and prescribed stretching surface heat flux (PHF). In this study, there are two methods to solve the non-linear differential equations are considered. In particular, the spectral relaxation method and Matlab programming language using bvp4c are used due to its simplicity for linearising and decoupling the non-linear differential equations system. The effects of radiation and mass transfer on unsteady MHD convective flow past a heated vertical plate in a porous medium with viscous dissolution as stated by Prasad and Reddy [30], where it was observed that, when the radiation parameter increase, the velocity and temperature decrease in the boundary layer. The thermal radiation effect on the flow and heat transfer impact is very crucial in the plan of numerous modern energy conversion system operating at a higher temperature. The thermal radiation surrounded by this system is regulated as a result of release by hot walls and the working fluid. In light of this matter, Jha [14] investigated hydromagnetic free convection and mass transfer flow past a uniformly accelerated moving vertical plate through a porous medium. The aim was to study the effects of magnetic field by assuming the magnetic lines of force to be fixed relative to fluid. Ibrahim et al. [11] examined unstable magneto-fluid dynamics flow of micro-polar fluid and heat transfer passing a vertical porous plate through a porous medium in the existence of thermal and mass diffusions with a stable heat source.

In the study of unsteady hydromagnetic chemically reacting mixed convection flow, the spectral relaxation method and the Matlab program bvp4c [[23], [35]], have been utilised to solve non-linear ordinary differential equations. In the boundary layer equations study, the equations capturing the system can be simplified by introducing similarity variables and expressing the flow properties in terms of the similarity variables. The outcome can be a system of non-linear ordinary equations. A new numerical method for solving non-linear systems of differential equations in the applications of boundary layer model was developed by motion [23]. This developed numerical method, called the spectral

relaxation method (SRM), is derived by re-organisation of the equations for the model presented in [23]. The spectral relaxation method and the Matlab program bvp4c have been used to solve various types of non-linear system problems such as non-linear equations arising in heat transfer [2].

1.2 Problem Statement

1.2.1 The main aim of the study

The main aim of this study is to analyse the effects of thermal radiation on the unsteady hydromagnetic chemically reacting mixed convection flow over a permeable stretching surface. Particularly, we want to study how the unsteady hydromagnetic convection flow will react chemically over a permeable stretching surface and also investigate the effects of unsteady hydromagnetic mixed convection with thermal radiation.

1.2.2 Objectives of the study

- To analyse the unsteady hydromagnetic chemically reacting mixed convection fluid flow using a numerical method called spectral relaxation method, and compare the results with those obtained using the in built solver bvp4c in matlab.
- To investigate the effects of slip and thermal radiation on unsteady hydromagnetic chemically reacting mixed convection fluid flow.
- To analyze the impacts of various parameters that affect the fluid flow over a permeable stretching embedded in a porous medium with thermal radiation and heat source/sink.

1.2.3 Hypothesis of the study

Permeable stretching sheet enclosed in a porous medium with thermal radiation and heat source/sink has an impact on the unsteady hydromagnetic chemically reacting mixed convection fluid flow.

1.2.4 Definitions of keywords

Magnetohydrodynamics (MHD) is the science of the movement of electrically conducting fluids beneath magnetic fields. MHD studies the undercurrents of the interaction of electrically conducting fluids and electromagnetic field. The fluid can be ionized gases (frequently called plasmas) or liquid metals. The fluid flow of an electrically conducting fluid under a magnetic field in all-purpose stretches rise to induced electric currents. The magnetic field applies mechanical forces on the induced electric currents. The induced electric currents fluid flow in the direction perpendicular to both magnetic field and the direction of motion of the fluid. However, the induced currents also generate their own magnetic field, which in turn disturbs the innovative magnetic field. [40].

Stretching sheet is a sheet which is stretched longer or wider without deprived of tearing or breaking. Stretching sheet problems are very imperative as their discoveries many practical applications in altered areas. Stretching sheet can be exponential, quadratically or linearly captured. At present, the study of shrinking sheet has received much attention due to its extraordinary behaviour in the field of fluid dynamics. Researchers are trying to exhibit different phenomena considering shrinking sheet in the different physical problems.[40].

Thermal radiation is energy transmission by the discharge of waves which convey energy away from the emitting object. Thermal radiation does not include an intervening medium to channel it. Thermal radiation characterizes a conversion of Thermal energy into electromagnetic energy. The characteristics of Thermal radiation are influenced by different properties of the surface emanating with its temperature, spectral absorptivity and spectral emissive power, as stated by Kirchhoff's law. The radiation is not monochromatic, that is, it does not entail of just a single frequency. Lastly, Thermal radiation ranges in wavelength from the longest infrared rays over the visible light spectrum to the shortest ultraviolet rays [40].

Mixed convection is the combination of forced and free convection, when the fluid

flow is reduced at the same time by both an outer and inner volumetric forces, by the density distribution of a fluid medium in a field of gravity. The most glowing demonstration of mixed convection is the apparent movement of the temperature bedded mass of air and water areas of the earth. Mixed convection is established in the systems of very small scales [42].

Chemical reaction is defined by a process that is characterized by a chemical reaction in which the initial materials are converted to products. Chemical changes entail the movement of electrons, influencing the formulation and breaking of chemical bonds [43].

Heat source/ sink defines the provisions or absorption of heat by anybody or device. Heat source defines the transfer of kinetic energy from one medium or object to a different or from an energy source to a medium or object, wherein such energy change can result in a system where heat will naturally move from high to low temperatures. A higher temperature is found in the heat source while low temperature is in the heat sink. There are many sorts of heat sources and the most natural form of heat will always be the solar heat [40].

Chapter 2

Literature Review

In this chapter, a literature review on the unsteady hydromagnetic chemically reacting mixed convection MHD fluid flow over a permeable stretching sheet embedded in a porous medium with thermal radiation and heat source/sink problem will be presented.

Many researchers have investigated the fluid dynamics problem using different approaches. Many researchers have been found that there are different results based on the choice parameters.

Uwanta and Hamza [31] investigated the unsteady hydromagnetic fluid flow of a reactive viscous fluid in a vertical channel with thermal diffusion, using unconditionally stable and convergent semi-implicit finite difference scheme, where they found that if the values of buoyancy parameter due to temperature (λ) increase, then both unsteady and steady-state velocity of the fluid increases. Furthermore, they discovered that if time increases, the velocity of the fluid increases until a steady-state condition is attained and they found that thermal diffusion, non-dimensional time, and temperature-dependent variable viscosity accelerates the fluid flow while the magnetic parameter retards the motion of the fluid.

Mitiku and Ponnane [20] studied the unsteady hydromagnetic chemically reacting assorted convection fluid flow over a porous stretching surface with slip and thermal radiation and they solved this problem numerically using an implicit finite difference method, termed the Keller box method. They found that if they increase the velocity fall away

parameter, then it reduces the fluid velocity and if the parameter of the temperature slip and species concentration slip parameter are raised so does the temperature and species concentration. They also found that if they improve the magnetic parameter (M) it influences the velocity of the fluid decreases, but it increases both temperature and species concentration. Increasing buoyancy forces ratio parameter and velocity slip parameter decreases the friction coefficient of the skin and assists fluid flow when $N>0$, the skin friction coefficient is less than the opposing fluid flow when $N>0$.

Makinde and Tshela [17] investigated the aspect of unsteady mixed convection with Soret and Dufour effects passing a porous plate of chemically changing fluid moving through a binary mixture. They used an iteration method together with fourth-order Runge-Kutta integration scheme and they found out that the local Nusselt number increases with increasing values of Dämkohler number, Soret number when the suction parameter is greater than zero and decreases with the increase in values of Schmidt number, radiation parameter and Dufour number. And also they found that the local Sherwood number increases with an increase in the values of Schmidt number, Radiation parameter, Dufour number (when $c>0$) and decreases with increasing values of Dämkohler number and Soret number. The problem of hydromagnetic fluid flow over an unsteady curved stretching surface is investigated by Naveed et. al. [26], the Runge-Kutta integration scheme was applied to demonstrate the shooting method to determine the fluid pressure and velocity. It was observed that the fluid velocity, and the momentum boundary surface thickness decrease for both parameters, that is, the magnetic parameter and the unsteadiness parameter. And also they discovered that the magnitude of the pressure distribution is decreased with an increase in the curvature and the unsteadiness. Patil et. al. [29] studied Dufour and Soret impacts on unsteady mixed convection fluid flow over the exponentially permeable stretching surface with a darcy-forchhiemer porous medium by using the Quasi-linearization method in conjunction with an implicit finite difference method. They discovered that the magnitude of velocity and temperature profiles decrease if one increases the stream-wise coordinate. Furthermore, they observed that the mixed convection parameter intensify the friction coefficient of the skin in accelerating fluid flow and reduces the friction in a decelerating fluid flow.

The production of heat, the emission of energy as electromagnetic waves and chemical reaction impacts on MHD mixed convection fluid flow over an unstable stretching permeable surface were investigated by Khan et. al. [15]. They used the shooting method called Nactsheim-Swigert as well as Runge-Kutta sixth order method. They learnt that the momentum and concentration thickness of the boundary layer decreases as suction parameter increases. Makinde and Tshehla [18], the unsteady hydromagnetic fluid flow of radiating fluid past a conventionally heated vertical plate,by using a partly discretization finite difference scheme linked with Runge-Kutta Fehlberg integration method. It was also established that both velocity and temperature profiles increase with time until the corresponding steady state is achieved for a given set of parameter values and the momentum boundary surface thickness increases as the values of Grashof number, Biot number and Eckert number increases, and decreases as the Hartmann's number, radiation parameter, Navier's slip parameter and Prandtl's number increases.

Seth et. al. [34] established that hydromagnetic natural convection fluid flow with heat and mass transfer of a chemically changing and heat sinking fluid through an accelerated moving vertical plate with increase in the level of temperature and surface concentration through a permeable medium by employing Laplace Transformation method. It was discovered that for both increased temperature plate with increased surface concentration and isothermal plate with uniform surface concentration, the magnetic field, heat absorption and chemical reaction have to decelerate influence on the fluid flow. Unsteady convective boundary layer fluid flow of an adhesive fluid at a vertical surface with variable fluid properties were investigated by Vajravelu et. al. [39] through the use of a Keller-box technique and determined that the thermal boundary layer is very thick in the case of suction as compared to the case of impermeability. Roslinda et. al. [28] studied the unsteady boundary layer fluid flow in the stagnation point area on a stretching sheet using the Keller-box method [26], and they established that if buoyancy parameter due to temperature (λ) is increasing, the thickness of the boundary layer decreases. Misra et. al. [19] investigated unsteady boundary layer fluid flow through a stretching plate and heat change with variable thermal conductivity and they used two methods to solve the heat fluid flow problems namely the prescribed stretching surface temperature and

stretching surface heat flux. In the case of PST, it was discovered that the Prandtl number is directly proportional to the Nusselt number but Nusselt number decreases as time increases and in the case of PHF, it was established that the Prandtl number could not be obtained from temperature field because of the thermal conductivity variation.

The impact of thermal radiation on an unstable heat and mass shift fluid flow of a chemically reacting fluid through a partly infinite vertical plate with glutinous dissolution was studied by Alao et. al. [3] through the use of the spectral relaxation method (SRM) and the results showed that an increase in Eckert number of the fluid actually increase the velocity and temperature profiles of the fluid flow. Nageeb et. al. [25] investigated heat and mass transfer in an unsteady MHD nanofluid boundary layer fluid flow due to a stretching surface by using the spectral relaxation method and they reported that the temperature and concentration profiles increase as the nanoparticle volume fraction values increases and thermophoresis parameter whereas the reverse trend was observed for the concentration profile with increase in the values of Brownian motion parameter.

The features of fluid flow, radiative heat and viscous fluid flow mass transfer over a permeable sheet stretching exponentially with Hall currents when there are heat generation and initial order chemical changing were studied by Mahaboobjan et. al. [16] using Runge-Kutta-Fehlberg scheme. They found that the radiation parameter and magnetic field produce thicker thermal boundary layers. Unsteady MHD boundary sheet stream with the dissemination of chemically reacting species experiencing initial order chemical response over a porous extending sheet with force or blowing and also with a power-law difference in wall concentration was explored by Bhattacharyya et. al. [7] by means of the quasi-linearization method. They found that the increase in magnetic parameter causes a decrease in velocity and an increase in concentration. Islam et. al. [13] investigated unsteady heat transmission of sticky incompressible boundary sheet fluid flow through an absorbent plate with the induced magnetic field by means of the explicit finite difference technique.

Ullah et. al. [38] investigated the problem of unsteady MHD assorted convection slip fluid flow of Casson fluid over non-linearly extending sheet embedded in a permeable medium

with chemical reaction, thermal radiation, heat source/sink and convective boundary conditions by using Keller-box method and they found that fluid velocity rises with increase in radiation parameter in the event of supporting fluid flow and it is contrary in the event of opposing fluid while radiation parameter has no effect on fluid velocity in the forced convection. Radiation and chemical response impacts on MHD thermosolutal nanofluid flow over a vertical plate in a holey medium were explored by Sulochana and Kishor [36] using bvp4c Matlab package and their results indicated that an increase in chemical response parameter improves the mass transmission rate.

Chapter 3

Problem Formulation

In this chapter, the partial differential equations of continuity, conservation of momentum, energy, and species concentration are derived.

3.1 Derivation of equations

We also outline the system of partial differential equations for the study. A similar system by Anderson [6] is given in the next subsection.

3.1.1 Derivation of Continuity equation

We model a volume V circumscribed by a surface S that is fixed in space. The mass inside was assumed by $\int_V \rho dv$, so the degree of diminution of mass in

$$\bar{V} = -\frac{\partial}{\partial t}\int_V \rho d\bar{V} = -\int_V \frac{\partial \rho}{\partial t} d\bar{V}, \tag{3.1}$$

if a mass is conserved, equation (3.1) must equivalent to the total rate of mass flux out of $\bar{V}$. The rate of external mass flux across any trivial element dS of S is ρdS where the degree of dS is identical to the component's area and we take dS along the external standard. Integrate over the whole surface we get the following: flux mass rate out of,

$$\bar{V} = \int_s \rho \bar{V} dS = \int_V \nabla\big(\rho \bar{V}\big) dv. \tag{3.2}$$

We applied Green's method to change to a volume integral. The integral $\nabla\big(\rho v\big)$ on the R.H.S is expressed in Cartesian coordinates $X = (x, y), \bar{V} = (u, v)$ as

$$\nabla \cdot \big(\rho \bar{V}\big) = \frac{\partial\big(\rho u\big)}{\partial x} + \frac{\partial\big(\rho v\big)}{\partial y}, \tag{3.3}$$

for mass to be conserved all over, equation (3.1) and (3.2) must be equal for any volume V and so we get the following continuity equation:

$$\frac{\partial \rho}{\partial t} + \nabla \cdot \big(\rho \bar{V}\big) = 0. \tag{3.4}$$

Note that for an incompressible fluid $\frac{\partial \rho}{\partial t} = 0$ always, so that the continuity equation for this fluid model reduces to $\nabla \bar{V} = 0$ where $\bar{V} = ui + vj$ and ρ is a constant, which is in Cartesian coordinates is:

$$\nabla \bar{V} = \frac{\partial u}{\partial x} + \frac{\partial v}{\partial y} = 0. \tag{3.5}$$

3.1.2 Derivation of Momentum equation

We consider a volume $\bar{V}$ confined by a material surface S that moves with the fluid flow, continuously containing identical material elements. Momentum is $\int_v dV \rho v$, so: Momentum change rate

$$\frac{d}{dt} \int_v d\bar{V} \rho v = \int_v d\bar{V} \rho \frac{D\bar{V}}{Dt}. \tag{3.6}$$

Note that the mass $\rho d\bar{V}$ of each material component is invariant. This must be equal to the net force on the element. In fact, there are two different kinds of forces that act on

any fluid, which are long oscillated outward body forces and short oscillated molecular forces. We introduce the stress tensor (τ), which is defined so the force applied per unit range transversely a surface element $dS \equiv \hat{n}ds$ (by the side fluid to which $\hat{n}$ points on the fluid on the other side) is $f = \tau\hat{n}$.

Total force (body force + surface force)

$$= \int_v d\bar{V}\rho g + \int_s \tau dS = \int_v d\bar{V}(\rho g + \nabla\tau). \tag{3.7}$$

With reference to Newton's second law, equation (3.6) and (3.7) must be equal for any V, so considering the Cauchy equation given as follows:

$$\rho\frac{D\bar{V}}{Dt} = \rho g + \nabla\tau. \tag{3.8}$$

Momentum, x:

$$\rho\frac{Du}{Dt} = \rho g_x + \frac{\partial}{\partial x}\tau_{xx} + \frac{\partial}{\partial y}\tau_{xy},$$

Momentum, y:

$$\rho\frac{Dv}{Dt} = \rho g_y + \frac{\partial}{\partial x}\tau_{yx} + \frac{\partial}{\partial y}\tau_{yy}.$$

where τ_{ij} is the force per unit area in the i direction across a plane with a standard in the j direction. Gradients in the tension tensor are required for there to be a net force on any component(consistent with the surface integral of $\tau\hat{n}$ equating to a capacity integral of $\nabla\tau$). It is possible to demonstrate that the tension tensor is symmetric, that is,

$$\tau_{xy} = \tau_{yx}. \tag{3.9}$$

The surface stress τ on any component arises after a mixture of pressure p and viscous friction μ, as given by the constitutive relations:

$$\tau_{xx} = -p + \lambda\nabla v + 2\mu\frac{\partial u}{\partial x}, \tag{3.10}$$

$$\tau_{yy} = -p + \lambda \nabla v + 2\mu \frac{\partial v}{\partial y}, \tag{3.11}$$

$$\tau_{xy} = \mu \left(\frac{\partial u}{\partial y} + \frac{\partial v}{\partial x} \right), \tag{3.12}$$

where μ and λ in equation (3.10), (3.11) and (3.12) represents the coefficients of dynamic and mass viscosity, respectively. In this work, we are very interested in equation (3.12) because our problem is two Dimensional.

We know that for incompressible fluid flow, $\nabla v = 0$ as shown in (3.5). Then the constitutive interactions reduce to,

$$\tau_{ij} = -p\delta_{ij} + \mu \left(\frac{\partial v_i}{\partial x_j} + \frac{\partial v_j}{\partial x_i} \right). \tag{3.13}$$

In this case, we use the notation $\mathbf{v} = (v_1, v_2)$, $\mathbf{x} = (x_1, x_2)$ and define the Kronecker delta symbol $\delta_{ij} = 1$ if $i = j$ and $\delta_{ij} = 0$ if $i \neq j$.

Momentum, x:

$$\rho \frac{Du}{Dt} = \rho g_x - \frac{\partial p}{\partial x} + \mu \left(\frac{\partial^2 u}{\partial x^2} + \frac{\partial^2 u}{\partial y^2} \right). \tag{3.14}$$

Momentum, y:

$$\rho \frac{Dv}{Dt} = \rho g_y - \frac{\partial p}{\partial y} + \mu \left(\frac{\partial^2 v}{\partial x^2} + \frac{\partial^2 v}{\partial y^2} \right). \tag{3.15}$$

Now we are going to use equation (3.10) because our problem is defined along the $x-$axis which is taken along the sheet in the vertically upward direction.

$$\rho \frac{Du}{Dt} = \rho g_x - \frac{\partial p}{\partial x} + \mu \left(\frac{\partial^2 u}{\partial x^2} + \frac{\partial^2 u}{\partial y^2} \right). \tag{3.16}$$

From material derivative we know that:

$$\frac{Du}{Dt} = \frac{\partial u}{\partial t} + (v \cdot \nabla) u = \frac{\partial u}{\partial t} + u \frac{\partial u}{\partial x} + v \frac{\partial u}{\partial y} \tag{3.17}$$

Now substituting equation (3.17) into (3.16) we get the following equation,

$$\rho \left[\frac{\partial u}{\partial t} + u \frac{\partial u}{\partial x} + v \frac{\partial u}{\partial y} \right] = \rho g_x - \frac{\partial p}{\partial x} + \mu \left(\frac{\partial^2 u}{\partial x^2} + \frac{\partial^2 u}{\partial y^2} \right). \tag{3.18}$$

Based on our problem the y component viscosity is high $\frac{\partial^2 u}{\partial y^2} >> 1$ and the x component viscosity is very small $\frac{\partial^2 u}{\partial x^2 << 1}$, equation (3.18) reduces to,

$$\rho\left[\frac{\partial u}{\partial t}+u\frac{\partial u}{\partial x}+v\frac{\partial u}{\partial y}\right]=\rho g_x-\frac{\partial p}{\partial x}+\mu\frac{\partial^2 u}{\partial y^2}. \tag{3.19}$$

Since pressure gradient is neglected then $\frac{\partial p}{\partial x}=0$. Now equation (3.19) becomes:

$$\rho\left[\frac{\partial u}{\partial t}+u\frac{\partial u}{\partial x}+v\frac{\partial u}{\partial y}\right]=\rho g_x+\mu\frac{\partial^2 u}{\partial y^2}. \tag{3.20}$$

Since g_x is the only body force which is gravity, then we set $g_x = g$ equation (3.20) is reduced to,

$$\rho\left[\frac{\partial u}{\partial t}+u\frac{\partial u}{\partial x}+v\frac{\partial u}{\partial y}\right]=\rho g+\mu\frac{\partial^2 u}{\partial y^2}. \tag{3.21}$$

For an ordinary convection problem, it is often assumed that the fluid is incompressible apart from the first term on the right-hand side of equation (3.21), this referred to as the Boussinesq hypothesis. The mass of a mixture is a function of temperature and species concentration. It can be expressed as a Tylor series near the neighbourhood of a reference point $(\bar{T}, \bar{C}_1, \bar{C}_2, ...\bar{C}_N)$ as shown by Naveed et al[25].

$$\rho=\bar{p}+\frac{\partial p}{\partial T}\left(T-\bar{T}\right)+\sum_{i=1}^{N}\frac{\partial p}{\partial C_i}\left(C_i-\bar{C}_i\right)+..... \tag{3.22}$$

We assume that $\bar{T}=T_\infty$ and $\bar{C}=C_\infty$.

Therefore,

$$\rho-\bar{p}=\frac{\partial p}{\partial T}\left(T-T_\infty\right)+\frac{\partial p}{\partial C}\left(C-C_\infty\right). \tag{3.23}$$

We know that $\rho=\bar{p}$, therefore, $\rho-\bar{p}=0$ if $\rho-\bar{p}$. Therefore, equation (3.23) becomes,

$$\rho=\frac{\partial p}{\partial T}\left(T-T_\infty\right)+\frac{\partial p}{\partial C}\left(C-C_\infty\right). \tag{3.24}$$

Substituting equation (3.24) into equation (3.21) on the right hand side we get the following,

$$\rho=g\left[\frac{\partial p}{\partial T}\left(T-T_\infty\right)+\frac{\partial p}{\partial C}\left(C-C_\infty\right)\right]+\mu\frac{\partial^2 u}{\partial y^2}.$$

Introducing the magnetic field intensity $B(t)$ which is moving downward, into the above equation

$$\rho\left[\frac{\partial u}{\partial t}+u\frac{\partial u}{\partial x}+v\frac{\partial u}{\partial y}\right]=g\frac{\partial p}{\partial T}\left(T-T_{\infty}\right)+g\frac{\partial p}{\partial C}\left(C-C_{\infty}\right)+\mu\frac{\partial^2 u}{\partial y^2}-\sigma B^2(t)u \quad (3.25)$$

Dividing both side by fluid density (ρ) we get,

$$\frac{\partial u}{\partial t}+u\frac{\partial u}{\partial x}+v\frac{\partial u}{\partial y}=g\left[\left(\frac{\partial p}{\partial T}\right)\div\rho\right]\left(T-T_{\infty}\right)+g\left[\left(\frac{\partial p}{\partial C}\right)\div\rho\right]\left(C-C_{\infty}\right)+\frac{\mu}{\rho}\frac{\partial^2 u}{\partial y^2}-\frac{\sigma B^2(t)u}{\rho}, \quad (3.26)$$

where ρ is density at the reference point, $\beta_T=\left[\left(\frac{\partial p}{\partial T}\right)\div\rho\right]$ is the coefficient of thermal expansion, and $\beta_C=\left[\left(\frac{\partial p}{\partial C}\right)\div\rho\right]$ is the composition coefficient of volume expansion. We let $\frac{\mu}{\rho}=\nu$, Therefore equation (3.26) becomes,

$$\frac{\partial u}{\partial t}+u\frac{\partial u}{\partial x}+v\frac{\partial u}{\partial y}=\nu\frac{\partial^2 u}{\partial y^2}+g\beta_T\left(T-T_{\infty}\right)+g\beta_C\left(C-C_{\infty}\right)-\frac{\sigma B^2(t)u}{\rho}. \quad (3.27)$$

3.1.3 Derivation of Energy equation

The energy equation is derived based on the physical law that the energy change rate in material particle = rate that energy is established by heat and work transmissions by that element, and at this instance the net rate of work done by pressure in the x-direction is given by

$$\left[up-\left(up+\frac{\partial(up)}{\partial x}dx\right)\right]dy=\frac{\partial(up)}{\partial x}dxdy. \quad (3.28)$$

In the same way, the net rate of work done by the shear tensions in the x-direction is, given by,

$$\left[\left(u\tau_{yx}+\frac{\partial u\tau_{yx}}{\partial y}dy\right)-u\tau_{yx}\right]=-\frac{\partial(u\tau_{yx})}{\partial y}dxdy. \quad (3.29)$$

By bearing in mind all the surface force, the work done on the moving fluid element due to these forces is merely,

$$\left[-\frac{\partial up}{\partial x}+\frac{\partial u\tau_{xx}}{\partial x}+\frac{\partial u\tau_{yx}}{\partial y}\right]dxdy. \tag{3.30}$$

Let us turn our attention to the degree at which heat receives energy. By assuming that the mass of the moving fluid element is $\rho dxdy$, we obtain, the rate that energy is received by heat which is given by $\rho\dot{q}dxdy$

By considering x-direction, the net heat is reassigned into the fluid element by thermal conduction is,

$$\left[\dot{q}_x-(\dot{q}_x+\frac{\partial\dot{q}_x}{\partial x}dx)\right]dy=-\frac{\partial\dot{q}_x}{\partial x}dxdy. \tag{3.31}$$

Now taking into account the heat transfer in y-direction, we obtain the following, Heating of the fluid element by

$$\left(\frac{\partial\dot{q}_x}{\partial x}+\frac{\partial\dot{q}_y}{\partial x}\right)dxdy.$$

The rate at which energy is received by heat is given by equation (3.31) the following equation,

$$\rho\dot{q}-\left(\frac{\partial\dot{q}_x}{\partial x}+\frac{\partial\dot{q}_y}{\partial y}\right)dxdy. \tag{3.32}$$

Heat transmission in the x and y directions in relation to the local temperature by current conduction, is given respectively by.

$$\begin{aligned}\dot{q}_x&=-K^*\tfrac{\partial T}{\partial x}\\ \dot{q}_y&=-K^*\tfrac{\partial T}{\partial y},\end{aligned} \tag{3.33}$$

where K^* is the thermal conductivity. Hence, by substituting equation (3.33) into (3.32) we obtain the following,

$$\left[\rho\dot{q}+\frac{\partial}{\partial x}(K^*+\frac{\partial T}{\partial x})+\frac{\partial}{\partial y}\left(K^*\frac{\partial T}{\partial y}\right)\right]dxdy, \tag{3.34}$$

and to obtain the rate of work which is transferred by a particle we say,

$$\rho\frac{D}{Dt}(e+\frac{v^2}{2})dxdy, \tag{3.35}$$

$$\rho\frac{D}{Dt}(e+\frac{v^2}{2}) = \rho\dot{q}+\frac{\partial}{\partial x}(K^*+\frac{\partial T}{\partial x})+\frac{\partial}{\partial y}(K^*\frac{\partial T}{\partial y})-\frac{\partial up}{\partial x}-\frac{\partial vp}{\partial y}+\frac{\partial u\tau_x x}{\partial x} \\ +\frac{\partial u\tau_y x}{\partial y}+\frac{\partial v\tau_x y}{\partial x}+\frac{\partial v\tau_y y}{\partial y}+\rho\bar{f}\bar{v}, \tag{3.36}$$

From equation (3.36) setting $\frac{v^2}{2}=0$ implies that

$$\rho\frac{De}{Dt} = \frac{\partial\rho e}{\partial t}+\nabla(\rho e\bar{v}). \tag{3.37}$$

Since the fluid flow is unsteady and $e = C_pT$ for a callorically perfect gas (C_p constant specific heat) we obtain the following using material derivative,

$$\rho\frac{De}{Dt} = \nabla\left(\rho C_pT\bar{v}\right) = C_p\rho\left[\frac{\partial T}{\partial t}+u\frac{\partial T}{\partial x}+v\frac{\partial T}{\partial y}\right]. \tag{3.38}$$

Now by substituting equation (3.38) into (3.36) we get the following,

$$C_p\rho\left[\frac{\partial T}{\partial t}+u\frac{\partial T}{\partial x}+v\frac{\partial T}{\partial y}\right] = \rho\dot{q}+\frac{\partial}{\partial x}(K^*\frac{\partial T}{\partial x})+\frac{\partial}{\partial y}\left(K^*\frac{\partial T}{\partial y}\right)-p\left(\frac{\partial u}{\partial x}+\frac{\partial v}{\partial y}\right) \\ +\lambda\left(\frac{\partial u}{\partial x}+\frac{\partial v}{\partial y}\right)^2+2\mu\left[(\frac{\partial u}{\partial x})^2+\left(\frac{\partial v}{\partial y}\right)^2\right] \tag{3.39}$$

Since the fluid flow occurs in the $y-$ direction, and is fixed in the $x-$ direction, $\frac{\partial}{\partial x}\left(K^*\frac{\partial T}{\partial x}\right)=\lambda\left(\frac{\partial u}{\partial x}\right)^2=0$ and also

$$2\mu\left[(\frac{\partial u}{\partial x})^2+\left(\frac{\partial v}{\partial y}\right)^2\right], \tag{3.40}$$

is neglected because of slip effects on the wall which implies that,

$$C_p\rho\left[\frac{\partial T}{\partial t}+u\frac{\partial T}{\partial x}+v\frac{\partial T}{\partial y}\right] = \rho\dot{q}+K^*\frac{\partial^2 T}{\partial y^2}+\lambda\left(\frac{\partial u}{\partial y}\right)^2. \tag{3.41}$$

Since the unsteady fluid flow starts at $t = 0$ then $\rho\dot{q} = 0$, (3.41) reduces to

$$C_p\rho\left[\frac{\partial T}{\partial t} + u\frac{\partial T}{\partial x} + v\frac{\partial T}{\partial y}\right] = K^*\frac{\partial^2 T}{\partial y^2} + \lambda\left(\frac{\partial u}{\partial y}\right)^2 \tag{3.42}$$

Adding radiative heat flux term and heat source effects on the temperature in equation, we obtain,

$$C_p\rho\left[\frac{\partial T}{\partial t} + u\frac{\partial T}{\partial x} + v\frac{\partial T}{\partial y}\right] = K^*\frac{\partial^2 T}{\partial y^2} + \lambda\left(\frac{\partial u}{\partial y}\right)^2 - \frac{\partial q_r}{\partial y} + Q_0(T - T_\infty), \tag{3.43}$$

Now by dividing equation (3.43) by $C_p\rho$ we get the following

$$\frac{\partial T}{\partial t} + u\frac{\partial T}{\partial x} + v\frac{\partial T}{\partial y} = \frac{K^*}{C_p\rho}\frac{\partial^2 T}{\partial y^2} + \frac{\lambda}{C_p\rho}(\frac{\partial u}{\partial y})^2 - \frac{1}{C_p\rho}\frac{\partial q_r}{\partial y} + \frac{Q_0}{C_p\rho}(T - T_\infty), \tag{3.44}$$

Setting $\frac{K^*}{C_p\rho} = \alpha$ and $\frac{\lambda}{C_p\rho} = \nu$, then

$$\frac{\partial T}{\partial t} + u\frac{\partial T}{\partial x} + v\frac{\partial T}{\partial y} = \alpha\frac{\partial^2 T}{\partial y^2} + \nu\left(\frac{\partial u}{\partial y}\right)^2 - \frac{1}{C_p\rho}\frac{\partial q_r}{\partial y} + \frac{Q_0}{C_p\rho}(T - T_\infty). \tag{3.45}$$

3.1.4 Derivation of Species concentration equation

The integral conservation of mass species equation is,

$$\frac{\partial}{\partial t}\int_V \rho_i dv + \int_A \rho_i(V_{rel}\cdot n)dA = -\int_A J_i n dA + \int_V \dot{m}_i''' dV$$

In the above equation, the surface integral may be transformed to volume integral by applying, $\int_A \Omega n dA = \int_V \nabla\Omega dV$ as follows,

$$\int_A \rho_i(V_{rel}\cdot n)dA = \int_V \nabla\cdot\rho_i V_{rel} dV, \tag{3.46}$$

$$\int_A J_i n dA = \int_V \nabla . J_i dV. \tag{3.47}$$

Substituting equation (3.45) and (3.46) into the integral conservation of mass species equation and considering

$$\frac{d}{dt}\int_V \rho\phi dv = \int_V \frac{\partial(\rho\phi)}{\partial t} dV,$$

the whole left-hand side of the integral conservation of mass species equation is included in a single volume integral that is,

$$\int_V \left(\frac{\partial \rho_i}{\partial t} + \nabla \cdot \rho_i V_{rel} + \nabla \cdot J_i - \dot{m}_i''' \right) dV = 0. \tag{3.48}$$

The integrand must equal zero for equation (3.48) to be true regardless of the shape and site of the control volume, that is,

$$\frac{\partial \rho_i}{\partial t} + \nabla \rho_i V_{rel} = -\nabla J_i + \dot{m}_i'''. \tag{3.49}$$

where $i = 1, 2, 3....., N$

The first term on the left-hand side of the equation models the species mass increase rate i per unit volume, and the second term captures the mass additions rate of the i^{th} species per unit volume by convection. The terms on the right-hand side are the net mass rate of i^{th} species per unit volume by dissemination, and rate of creation of species i by chemical reaction. After defining the mass fraction of species i as

$$\omega_i = \frac{\rho_i}{\rho},$$

equation (3.48) can be written as

$$\left[\frac{\partial \rho}{\partial t} + \nabla . \rho V_{rel} \right] \omega_i + \rho \left[\frac{\partial \omega_i}{\partial t} + \nabla \omega_i V_{rel} \right] = -\nabla J_i + \dot{m}_i'''. \tag{3.50}$$

According to the continuity equation,

$$\frac{\partial \rho}{\partial t} + \nabla \rho V_{rel} = 0$$

the bracket on the left-hand side of equation (3.49) is zero. The second bracket on the left-hand side is the substantial derivative of the mass fraction. Therefore, the conservation of species mass in terms of mass fraction becomes,

$$\rho\frac{D\omega_i}{Dt} = -\nabla.J_i + \dot{m}_i''' \tag{3.51}$$

Assuming binary system of A and B, one can use Fick's law in equation (3.50) to yield.

$$\rho\frac{D\omega_A}{Dt} = -\rho\nabla(D_{AB}\nabla_{\omega A}) + \dot{m}_A'''. \tag{3.52}$$

Which is useful in determining the diffusion in dilute liquid solution at constant temperature and pressure. Equation (3.51), with $\dot{m}_A''' = 0$, is similar to energy equation with no internal heat source and viscous dissipation,

$$\rho C_p\frac{DT}{Dt} = \nabla.(k\nabla T) + q''' + \nabla V_{rel}, \tau_{rel}.$$

and therefore it is used for analogy between heat and mass transfer analysis.
In the discussion to develop equation (3.48), the mass fraction and mass flux were used. The species equation can also be developed in terms of molar concentration and molar flux. By following a similar procedure, the species equation is,

$$\frac{\partial C_i}{\partial t} = -\nabla\cdot\dot{n}_i'' + \dot{n}_i'''. \tag{3.53}$$

where the molar flux relative to the stationary coordinate axes can be obtained.

$$\dot{m}_i'' = \rho_i\bar{V} + J_i = \omega_i\sum_{j=1}^{N}\dot{m}_j'' + J_i.$$

that is,

$$\dot{n}_i'' = c_i\bar{V}^* + J_i^*. \tag{3.54}$$

Substituting equation (3.53) into (3.52), we have

$$\frac{\partial c_i}{\partial t} + \nabla(c_i\bar{V}^*) = -\nabla J_i^* + \dot{n}_i'''. \tag{3.55}$$

where the first term on the left-hand side is rate of increase of mole of the species j per unite volume, and the second term is net rate of additions of mole of the i^{th} species per unit volume by convection.The terms on the right-hand side are net rate of mole of i^{th} species per unit volume by diffusion, and the molar rate of production of species i by chemical reaction. for a binary system of components A and B with constant pressure, equation (3.54) reduces to,

$$\frac{\partial C}{\partial t} + \nabla \cdot (c\bar{V}^*) = -c\nabla \cdot (D\nabla) + \dot{n}'''. \tag{3.56}$$

where c is the mixture molar concentration and $\bar{V}^*$ is molar-averaged velocity. Equation (3.55) can be applied to low density gases with constant temperature and pressure.
By considering left-hand side of equation (3.55) using material derivative.

$$\frac{\partial C}{\partial t} + \bar{V}.(c.\nabla)$$

where $\bar{V} = (u, v)$

$$\frac{\partial C}{\partial t} + \bar{V}.(c.\nabla) = \frac{\partial C}{\partial t} + u\frac{\partial C}{\partial x} + v\frac{\partial C}{\partial y}, \tag{3.57}$$

And also considering right-hand side of equation (3.55)

$$-c\nabla \cdot (D\nabla) + \dot{n}''', \tag{3.58}$$

where,

$$\dot{n}''' = K(C - C_\infty) \tag{3.59}$$

By substituting equation (3.58) into equation (3.57) we have

$$-D\nabla^2 c + K(C - C_\infty) = -D\left[\frac{\partial^2 C}{\partial x^2} + \frac{\partial^2 C}{\partial y^2}\right] + K(C - C_\infty). \tag{3.60}$$

Since we are considering $y-$component the $\frac{\partial^2 C}{\partial x^2}$ is neglected then

$$D\frac{\partial^2 C}{\partial y^2} - K(C - C_\infty). \tag{3.61}$$

By combining equation (3.56) and (3.60) we have,

$$\frac{\partial C}{\partial t} + u\frac{\partial C}{\partial x} + v\frac{\partial C}{\partial y} = D\frac{\partial^2 C}{\partial y^2} - K(C - C_\infty). \tag{3.62}$$

3.2 Summary

Continuity equation

$$\frac{\partial u}{\partial x} + \frac{\partial v}{\partial y} = 0$$

Momentum equation

$$\frac{\partial u}{\partial t} + u\frac{\partial u}{\partial x} + v\frac{\partial u}{\partial y} = \nu\frac{\partial^2 u}{\partial y^2} + g\beta_T\left(T - T_\infty\right) + g\beta_C\left(C - C_\infty\right) - \frac{\sigma B^2(t)u}{\rho}$$

Energy equation

$$\frac{\partial T}{\partial t} + u\frac{\partial T}{\partial x} + v\frac{\partial T}{\partial y} = \alpha\frac{\partial^2 T}{\partial y^2} + \nu\left(\frac{\partial u}{\partial y}\right)^2 - \frac{1}{C_p\rho}\frac{\partial q_r}{\partial y} + \frac{Q_0}{C_p\rho}(T - T_\infty)$$

Species concentration equation

$$\frac{\partial C}{\partial t} + u\frac{\partial C}{\partial x} + v\frac{\partial C}{\partial y} = D\frac{\partial^2 C}{\partial y^2} - K(C - C_\infty)$$

The boundary conditions are,

At $y = 0$,

$$u = U_w(x,t), v = V_w(t), T = T_w(x,t), C = C_w(x,t) \tag{3.63}$$

As $y \longrightarrow \infty$,

$$u \longrightarrow 0, T \longrightarrow T_\infty, C \longrightarrow C_\infty \tag{3.64}$$

The terms u and v in the above expression denote velocity components in the x and y direction respectively, T and T_infty is the fluid temperature near the wall and the fluid

temperature which is far away from the wall, C and C_infty are species concentration near the surface and species concentration which is far from the surface, nu is the kinematic thickness, g is the acceleration due to gravity, $beta_T$ and $beta_C$ are volumetric coefficient of thermal expansion and volumetric coefficient of concentration expansion, $sigma$ is the electrical conductivity of the fluid, rho is the density of the fluid, $alpha$ is the thermal diffusivity, c_p is the specific heat capacity, q_r is the radiative heat flux, D is the mass diffusivity of the species concentration, k is the chemical reaction and B is the transverse magnetic field strong point.

Chapter 4

Transformation Method

In this chapter, we are going to use a transformation method to transform partial differential equations into ordinary differential equations.

The governing partial differential equations (3.5), (3.27), (3.45) and (3.62) can be decreased to a set of ordinary differential equations on introducing the following similarity variables [41],

$$\eta = y\left(\frac{a}{\nu(1-ct)}\right)^{\frac{1}{2}}, \quad \psi(x,y,t) = \left(\frac{\nu a}{(1-ct)}\right)^{\frac{1}{2}} x f(\eta), \quad \theta(\eta) = \frac{T-T_\infty}{T_w-T_\infty},$$

$$\phi(\eta) = \frac{C-C_\infty}{C_w-C_\infty}, \quad u = \frac{\partial \psi}{\partial y}, \quad v = -\frac{\partial \psi}{\partial x},$$

$$\frac{\partial \eta}{\partial y} = \left(\frac{a}{\nu(1-ct)}\right)^{\frac{1}{2}} \tag{4.1}$$

$$\left.\begin{aligned}
\frac{\partial \eta}{\partial t} &= \frac{y a^{\frac{1}{2}}}{\nu^{\frac{1}{2}}}\left(\frac{-1}{2}\right)(1-ct)^{\frac{-3}{2}}(-c), \\
&= \frac{y a^{\frac{1}{2}}}{\nu^{\frac{1}{2}}}(1-ct)^{\frac{-1}{2}}\left[\frac{c}{2}(1-ct)^{-1}\right], \\
&= \eta \times \frac{c}{2(1-ct)}, \\
&= \frac{\eta c}{2(1-ct)}
\end{aligned}\right\} \tag{4.2}$$

$$\psi(x,y,t) = \left(\frac{\nu a}{(1-ct)}\right)^{\frac{1}{2}} x f(\eta), \qquad u = \frac{\partial \psi}{\partial y} \tag{4.3}$$

$$\left.\begin{aligned}
\frac{\partial \psi}{\partial y} &= \left(\frac{\nu a}{1-ct}\right)^{\frac{1}{2}} x f'(\eta)\frac{\partial \eta}{\partial y} \\
&= \left(\frac{\nu a}{1-ct}\right)^{\frac{1}{2}} x f'(\eta)\left(\frac{a}{\nu(1-ct)}\right)^{\frac{1}{2}} \\
&= \sqrt{\frac{a^2}{(1-ct)^2}} x f'(\eta) = \frac{a}{1-ct} x f'(\eta) \\
u &= \frac{a}{1-ct} x f'(\eta)
\end{aligned}\right\} \tag{4.4}$$

$$\left.\begin{aligned}
v &= -\frac{\partial \psi}{\partial x}, \qquad \frac{\partial \psi}{\partial x} = \frac{\partial}{\partial x}\left[\left(\frac{\nu a}{1-ct}\right)^{\frac{1}{2}} x f'(\eta)\right] \\
u &= -\left[\left(\frac{\nu a}{1-ct}\right)^{\frac{1}{2}} f(\eta) + \left(\frac{\nu a}{1-ct}\right)^{\frac{1}{2}} x f'(\eta)\frac{\partial \eta}{\partial x}\right], \\
u &= -\left[\left(\frac{\nu a}{1-ct}\right)^{\frac{1}{2}} f(\eta) + \left(\frac{\nu a}{1-ct}\right)^{\frac{1}{2}} x f'(\eta)0\right], \\
v &= -\left(\frac{\nu a}{1-ct}\right)^{\frac{1}{2}} f(\eta)
\end{aligned}\right\} \tag{4.5}$$

4.1 Similarity Transformation

In this section we are going to use the above similarity variables to transform partial differential equations of continuity, momentum, heat and concentration, respectively.

4.1.1 Similarity transformation for continuity equation:

$$\frac{\partial u}{\partial x}+\frac{\partial v}{\partial y}=0$$

$$u=\frac{a}{1-ct}xf'(\eta)$$

$$\frac{\partial u}{\partial x}=\frac{\partial}{\partial x}\left(\frac{a}{1-ct}xf'(\eta)\right)$$

$$\frac{a}{1-ct}f'(\eta)+\frac{a}{1-ct}xf''(\eta)\frac{\partial \eta}{\partial x}=\frac{a}{1-ct}f'(\eta)+0,\Rightarrow \frac{\partial u}{\partial x}=\frac{a}{1-ct}f'(\eta) \tag{4.6}$$

$$v=-\left(\frac{\nu a}{1-ct}\right)^{\frac{1}{2}}f(\eta)\Rightarrow \frac{\partial v}{\partial y}=-\left(\frac{\nu a}{1-ct}\right)^{\frac{1}{2}}f'(\eta)\frac{\partial \eta}{\partial y}=-\left(\frac{\nu a}{1-ct}\right)^{\frac{1}{2}}f'(\eta)\left(\frac{a}{\nu(1-ct)}\right)^{\frac{1}{2}}$$

$$=\sqrt{\frac{\nu a^2}{\nu(1-ct)^2}}f'(\eta)$$

Therefore:

$$\frac{\partial v}{\partial y}=-\frac{a}{1-ct}f'(\eta) \tag{4.7}$$

$$\frac{\partial u}{\partial x}+\frac{\partial v}{\partial y}=\frac{a}{1-ct}f'(\eta)-\frac{a}{1-ct}f'(\eta)=0$$

Satisfies the continuity equation (3.5)

4.1.2 Similarity transformation for momentum equation:

$$\frac{\partial u}{\partial t}+u\frac{\partial u}{\partial x}+v\frac{\partial u}{\partial y}=\nu\frac{\partial^2 u}{\partial y^2}+g\beta_T(T-T_\infty)+g\beta_C(C-C_\infty)-\frac{\sigma B^2(t)}{\rho}u$$

$$\frac{\partial \eta}{\partial y}=\left(\frac{a}{\nu(1-ct)}\right)^{\frac{1}{2}},\quad y=\eta\left(\frac{a}{\nu(1-ct)}\right)^{-\frac{1}{2}} \tag{4.8}$$

$$\eta=y\left(\frac{a}{\nu(1-ct)}\right)^{\frac{1}{2}}\Rightarrow \frac{\partial \eta}{\partial t}=\frac{1}{2}y\left(\frac{a}{\nu(1-ct)}\right)^{-\frac{1}{2}}\frac{ac}{\nu(1-ct)^2}$$

$$= \frac{1}{2}\eta\left(\frac{a}{\nu(1-ct)}\right)^{-\frac{1}{2}}\left(\frac{a}{\nu(1-ct)}\right)^{-\frac{1}{2}}\frac{-ac}{\nu(1-ct)^2} = \frac{1}{2}\frac{n}{\frac{a}{\nu(1-ct)}}\frac{-ac}{\nu(1-ct)^2} = \frac{1}{2}\eta\frac{\nu(1-ct)}{a}\frac{ac}{\nu(1-ct)^2}$$

$$= \frac{1}{2}\eta\frac{\nu(1-ct)}{a}\frac{ac}{\nu(1-ct)^2}$$

Therefore,

$$\frac{\partial\eta}{\partial t} = \frac{\eta c}{2(1-ct)}$$

$$\frac{\partial u}{\partial t} = \frac{(0)(1-ct)-a(-c)}{(1-ct)^2}xf'(\eta) + \frac{a}{1-ct}xf''(\eta)\frac{\partial\eta}{\partial t}$$

$$= \frac{ac}{(1-ct)^2}xf'(\eta) + \frac{a}{1-ct}xf''(\eta)\frac{1\eta c}{2(1-ct)}$$

Therefore,

$$\frac{\partial u}{\partial t} = \frac{ac}{(1-ct)^2}xf'(\eta) + \frac{ac\eta}{2(1-ct)^2}xf''(\eta) \tag{4.9}$$

$$\frac{\partial u}{\partial x} = \frac{a}{1-ct}f'(\eta) + \frac{a}{1-ct}xf''(\eta)\frac{\partial\eta}{\partial x}, \qquad = \frac{a}{1-ct}f'(\eta) + \frac{a}{1-ct}xf''(0)$$

Therefore,

$$\frac{\partial u}{\partial x} = \frac{a}{1-ct}f'(\eta) \tag{4.10}$$

$$u\frac{\partial u}{\partial x} = \frac{a}{1-ct}xf'(\eta)\frac{a}{1-ct}f'(\eta) = \frac{a^2}{(1-ct)^2}x(f')^2(\eta) \tag{4.11}$$

$$\frac{\partial u}{\partial y} = \frac{a}{1-ct}xf''(\eta)\frac{\partial\eta}{\partial y}$$

Therefore,

$$\frac{\partial u}{\partial y} = \frac{a}{1-ct}xf'(\eta)\left(\frac{a}{\nu(1-ct)}\right)^{\frac{1}{2}} \tag{4.12}$$

$$v\frac{\partial u}{\partial y} = -\left(\frac{\nu a}{1-ct}\right)^{\frac{1}{2}}\frac{a}{1-ct}xf''(\eta)\left(\frac{a}{\nu(1-ct)}\right)^{\frac{1}{2}}$$

Therefore,

$$v\frac{\partial u}{\partial y} = \frac{a^2}{(1-ct)^2}xf''(\eta)f(\eta) \tag{4.13}$$

$$\frac{\partial^2 u}{\partial y^2} = \frac{\partial}{\partial y}\left(\frac{\partial u}{\partial y}\right) = \frac{\partial}{\partial y}\left[\frac{a}{1-ct}xf''(\eta)\left(\frac{a}{\nu(1-ct)}\right)^{\frac{1}{2}}\right]$$

$$= \frac{a}{1-ct}xf'''(\eta)\left(\frac{a}{\nu(1-ct)^{\frac{1}{2}}}\right)\frac{\partial \eta}{\partial y} = \frac{a}{1-ct}xf'''(\eta)\left(\frac{a}{\nu(1-ct)^{\frac{1}{2}}}\right)\left(\frac{a}{\nu(1-ct)^{\frac{1}{2}}}\right)$$

Therefore,

$$\frac{\partial^2 u}{\partial y^2} = \frac{a^2}{\nu(1-ct)^2}xf'''(\eta), \qquad \nu\frac{\partial^2 u}{\partial y^2} = \frac{\nu a^2 x}{\nu(1-ct)^2}f'''(\eta) \tag{4.14}$$

$$\nu\frac{\partial^2 u}{\partial y^2} = \frac{a^2 x}{(1-ct)^2}f'''(\eta), \quad \theta(T_w - T_\infty) = T - T_\infty, \quad \phi(C_w - C_\infty) = C - C_\infty. \tag{4.15}$$

$$\frac{ac}{(1-ct)^2}xf'(\eta) + \frac{a\eta c}{2(1-ct)^2}xf''(\eta) + \frac{a^2}{(1-ct)^2}xf'^2(\eta)$$
$$+\frac{a^2}{(1-ct)^2}xf(\eta)f''(\eta) = \frac{a^2}{(1-ct)^2}xf'''(\eta) + g\beta_T\theta(T_w - T_\infty)$$
$$+g\beta_C\phi(C_w - C_\infty) - \frac{\sigma B_0}{\rho\sqrt{1-ct}}\frac{B_0}{\sqrt{1-ct}}\frac{a}{1-ct}xf'(\eta)$$

Multiplying by $\frac{(1-ct)^2}{a^2x}$ both side we get the following,

$$f''' + f''f - \frac{B_0^2}{a\rho}f' - f'^2 - \frac{a}{c}f' - \frac{1a}{2c}\eta$$
$$f'' + g\beta_T\theta(T_w - T_\infty)\frac{(1-ct)^2}{a^2x}\frac{L}{x} + g\beta_C\phi(C_w - C_\infty)\frac{(1-ct)^2}{a^2x}\frac{L}{x} = 0$$

We know that $M = \frac{\sigma(B_0)^2}{\rho a}$ and $A = \frac{c}{a}$ where M is the magnetic parameter and A is the unsteady parameter.

$$f''' + f''f - Mf' - f'^2 - A(f' + \frac{1}{2}\eta f'') + g\beta_T\theta(T_w - T_\infty)L\frac{(1-ct)^2}{a^2x^2} +$$
$$g\beta_C\phi(C_w - C_\infty)L\frac{(1-ct)^2}{a^2x^2} = 0$$

$$f''' + f''f - Mf' - f'^2 - A(f' + \frac{1}{2}\eta f'') + g\beta_T\theta(T_w - T_\infty)L\frac{L^2}{L^2}\frac{\nu^2}{\nu^2}\frac{1}{\frac{a^2x^2}{(1-ct)^2}}$$
$$+g\beta_C\phi(C_w - C_\infty)L\frac{L^2}{L^2}\frac{\nu^2}{\nu^2}\frac{1}{\frac{a^2x^2}{(1-ct)^2}} = 0$$

$$f''' + f''f - Mf' - f'^2 - A(f' + \frac{1}{2}\eta f'') + \frac{g\beta_T\theta(T_w - T_\infty)}{\nu^3}L^3\frac{\nu^2}{U_w^2L^2} + \frac{g\beta_C\phi(C_w - C_\infty)}{\nu^2}L^3\frac{\nu^2}{U_w^2L^2} = 0$$

$$f''' + f''f - Mf' - f'^2 - A(f' + \frac{1}{2}\eta f'') + \theta Gr\frac{1}{\frac{(U_wL}{\nu})^2} + \phi Gr^*\frac{1}{\frac{(U_wL}{\nu})^2} = 0$$

$$f''' + f''f - Mf' - f'^2 - A(f' + \frac{1}{2}\eta f'') + \theta\frac{Gr}{R_eL^2} + \phi\frac{Gr^*}{R_eL^2} = 0$$

$$f''' + f''f - Mf' - f'^2 - A(f' + \frac{1}{2}\eta f'') + \theta\lambda + \phi\lambda_1 = 0$$

4.1.3 Similarity transformation for energy equation:

$$\theta = \frac{T - T_\infty}{T_w - T_\infty}, \Rightarrow \theta(T_w - T_\infty) = T - T_\infty \Rightarrow T = \theta(T_w - T_\infty) + T_\infty$$

$$\frac{\partial T}{\partial t} = \frac{2bxc}{(1-ct)^3}\theta + \frac{\partial}{\partial t}\left(\theta(T_w - T_\infty) + T_\infty\right) = \frac{2bxc}{(1-ct)^3}\theta + (T_w - T_\infty)\frac{\partial\theta}{\partial\eta}\frac{\partial\eta}{\partial t}$$

$$= \frac{2bxc}{(1-ct)^3}\theta + (T_w - T_\infty)\theta' - \frac{1}{2}\frac{\eta c}{(1-ct)}$$

Therefore,

$$\frac{\partial T}{\partial t} = \frac{2bxc}{(1-ct)^3}\theta - \frac{1}{2}\frac{\eta c}{(1-ct)}(T_w - T_\infty)\theta' \tag{4.16}$$

$$\frac{\partial T}{\partial x} = \frac{\partial\left(\theta(T_w - T_\infty) + T_\infty\right)}{\partial x},$$

$$\frac{\partial T}{\partial x} = \frac{b}{(1-ct)^2}\theta$$

Therefore,

$$\frac{\partial T}{\partial x} = \frac{b}{(1-ct)^2}\theta \tag{4.17}$$

$$u\frac{\partial T}{\partial x} = \frac{a}{(1-ct)}xf'\frac{b}{(1-ct)^2}\theta = \frac{abx}{(1-ct)^3}\theta f' \tag{4.18}$$

$$\frac{\partial T}{\partial y} = \frac{\partial}{\partial y}\left(T_\infty + (T_w - T_\infty)\theta\right) = \frac{\partial}{\partial \eta}\left(T_\infty + (T_w - T_\infty)\theta\right)\frac{\partial \eta}{\partial y} = \left(\frac{a}{\nu(1-ct)}\right)^{\frac{1}{2}}(T_w - T_\infty)\theta'$$

$$v\frac{\partial T}{\partial y} = -(T_w - T_\infty)\theta'\left(\frac{\nu a}{1-ct}\right)^{\frac{1}{2}} f\left(\frac{a}{\nu(1-ct)}\right)^{\frac{1}{2}}$$

$$v\frac{\partial T}{\partial y} = -\frac{a}{1-ct}(T_w - T_\infty)f\theta', \tag{4.19}$$

$$\frac{\partial^2 T}{\partial y^2} = \frac{\partial}{\partial y}\left(\frac{\partial T}{\partial y}\right)$$

$$= \frac{\partial}{\partial y}\left((T_w - T_\infty)\theta'\right)\left(\frac{a}{\nu(1-ct)}\right)^{\frac{1}{2}} = (T_w - T_\infty)\frac{\partial \theta'}{\partial \eta}\frac{\partial \eta}{\partial y}\left(\frac{a}{\nu(1-ct)}\right)^{\frac{1}{2}}$$

$$= (T_w - T_\infty)\theta''\left(\frac{a}{\nu(1-ct)}\right)^{\frac{1}{2}}\left(\frac{a}{\nu(1-ct)}\right)^{\frac{1}{2}} = (T_w - T_\infty)\theta''\frac{a}{\nu(1-ct)} = \frac{a}{\nu(1-ct)}(T_w - T_\infty)\theta''$$

$$\alpha\frac{\partial^2 T}{\partial y^2} = (T_w - T_\infty)\theta''\frac{a\alpha}{\nu(1-ct)}$$

$$\alpha\frac{\partial^2 T}{\partial y^2} = \frac{a\alpha}{\nu(1-ct)}(T_w - T_\infty)\theta'' = -\frac{1}{\rho C_p}\frac{\partial q_r}{\partial y} \tag{4.20}$$

The radiative heat flux by using Rosseland approximation is written as,

$$q_r = -\frac{4\sigma^*}{3k^*}\frac{\partial T^4}{\partial y} \tag{4.21}$$

where σ^* is the Stefen-Boltzman constant and k^* is the absorption coefficient. T^4 may be linearly expanded in a Taylor's series about T_∞ to get

$$T_4 = T_\infty^4 + (T - T_\infty)f'(T_\infty) + \frac{(T-T_\infty)^2}{2!}f''(T_\infty) + \frac{(T-T_\infty)^3}{3!}f'''(T_\infty) + \frac{(T-T_\infty)^4}{4!}f^i v(T_\infty) + ...,$$

$$T^4 = T_\infty^4 + 4TT_\infty^3 - 4T_\infty^4 + 6T_\infty^2 + 6T_\infty^2(T^3 - 3T^2T_\infty - T_\infty^3) + ..., \tag{4.22}$$

and neglecting higher order terms beyond the first order degree in $(T - T_\infty)$, reduce to the following,

$$T^4 \cong 4TT_\infty^3 - 3T_\infty^4,$$

$$q_r = -\frac{16\sigma^* T_\infty^3}{3k^*}\frac{\partial^2 T}{\partial y^2}, \tag{4.23}$$

Since follows that,

$$\frac{\partial q_r}{\partial y} = \frac{16\sigma^* T_\infty^3}{3k^*}\frac{\partial^2 T}{\partial y^2}$$

$$-\frac{1}{\rho C_p}\frac{\partial q_r}{\partial y} = -\frac{1}{\rho C_p}\frac{16\sigma^* T_\infty^3}{3k^*}\frac{\partial^2 T}{\partial y^2}$$

$$\left(\frac{\partial u}{\partial y}\right)^2 = \left(\frac{a}{1-ct}xf''\frac{a}{\nu(1-ct)}^{\frac{1}{2}}\right)^2 = \frac{a^3}{\nu(1-ct)^3}x^2\left(f''\right)^2$$

$$\frac{\nu}{\rho C_p}\left(\frac{\partial u}{\partial y}\right)^2 = \frac{a^3}{\rho C_p(1-ct)^3}x^2\left(f''\right)^2 \tag{4.24}$$

$$\frac{Q_0}{\rho C_p}(T-T_\infty) = \frac{Q_0}{\rho C_p}(T_w - T_\infty)\theta, \qquad Q = \frac{Q_0(1-ct)}{\rho C_p a} \tag{4.25}$$

where Q is the local heat source/sink parameter. Make Q_0 the subject of the formula. Therefore,

$$Q_0 = \frac{\rho C_P a}{1-ct}Q$$

Substituting Q_0 into equation (4.25) then we get,

$$\frac{a}{1-ct}Q(T_w - T_\infty)\theta$$

$$\frac{\partial T}{\partial t} + u\frac{\partial T}{\partial x} + v\frac{\partial T}{\partial y} = \alpha\frac{\partial^2 T}{\partial y^2} - \frac{1}{\rho c_p}\frac{\partial q_r}{\partial y} + \frac{\nu}{\rho c_p}\left(\frac{\partial u}{\partial y}\right)^2 \pm \frac{Q_0}{\rho c_p}(T-T_\infty)$$

$$-\frac{1}{2}\frac{\eta c}{1-ct}(T_w - T_\infty)\theta' + \frac{bx}{(1-ct)^2}\frac{\nu}{\alpha(T_w-T_\infty)}\theta f' - \frac{a}{1-ct}(T_w-T_\infty)f\theta'$$
$$= \frac{a\alpha}{\nu(1-ct)}(T_w-T_\infty)\theta''$$
$$-\frac{1}{\rho C_p}\frac{16\sigma^* T_\infty^3}{3k^*}\frac{a}{\nu(1-ct)}(T_w-T_\infty)\theta'' + \frac{a^3x^2}{(1-ct)^3}\left(f''\right)^2 + \frac{a}{1-ct}Q(T_w-T_\infty)\theta$$

$$\frac{a\alpha}{\nu(1-ct)}(T_w-T_\infty)\theta''-\frac{1}{\rho C_p}\frac{16\sigma^*T_\infty^3}{3k^*}\frac{a}{\nu(1-ct)}(T_w-T_\infty)\theta''+\frac{a}{1-ct}(T_w-T_\infty)\theta'+\frac{1}{2}\frac{\eta c}{1-ct}(T_w-T_\infty)\theta'+\frac{a^3x^2}{\rho C_p(1-ct)^3}\left(f''\right)^2$$

$$\frac{\partial T}{\partial t}=\frac{2bxc}{(1-ct)^3}\theta-\frac{1}{2}\frac{\eta c}{1-ct}(T_w-T_\infty)\theta' \tag{4.26}$$

$$u\frac{\partial T}{\partial x}=\frac{abx}{(1-ct)^3}\theta f' \tag{4.27}$$

$$v\frac{\partial T}{\partial y}=-\frac{a}{1-ct}(T_w-T_\infty)f\theta' \tag{4.28}$$

$$\alpha\frac{\partial^2 T}{\partial y^2}=\frac{a\alpha}{\nu(1-ct)}(T_w-T_\infty)\theta'' \tag{4.29}$$

$$-\frac{1}{\rho C_p}\frac{\partial q_r}{\partial y}=-\frac{1}{\rho C_p}\frac{16\sigma^*T_\infty^3}{3k^*}\frac{a}{\nu(1-ct)}(T_w-T_\infty)\theta'' \tag{4.30}$$

$$\frac{\nu}{\rho C_p}\left(\frac{\partial u}{\partial y}\right)^2=\frac{a^3x^2}{\rho C_p(1-ct)^3}\left(f''\right)^2 \tag{4.31}$$

$$\frac{Q_0}{\rho C_p}(T-T_\infty)=\frac{a}{1-ct}Q(T_w-T_\infty)\theta \tag{4.32}$$

Multiply all equations from (4.26) to (4.32) by

$$\frac{\nu(1-ct)}{a\alpha(T_w-T_\infty)}$$

equation (4.26) becomes,

$$\frac{2bxc}{(1-ct)^3}\theta\frac{\nu(1-ct)}{a\alpha(T_w-T_\infty)}-\frac{1}{2}\frac{\eta c}{1-ct}(T_w-T_\infty)\theta'\frac{\nu(1-ct)}{a\alpha(T_w-T_\infty)}=\frac{2bxc}{(1-ct)^3}\theta-\frac{1}{2}\eta\frac{c}{a}\frac{\nu}{\alpha}\theta'$$

$$\frac{2bxc}{(1-ct)^3}\theta\frac{\nu(1-ct)}{a\alpha\left(T_{\infty+\frac{bx}{(1-ct)^2}}-T_\infty\right)}=\frac{2bxc}{a(1-ct)^2}\frac{\nu}{\alpha}\frac{(1-ct)^2}{bx}=2\frac{c}{a}\frac{\nu}{\alpha}\theta$$

where $\frac{c}{a}=A$ is the unsteady parameter and $\frac{\nu}{\alpha}=Pr$ is the Prandtl number

Therefore we get,

$$2APr\theta-\frac{1}{2}\eta APr\theta'=APr\left(2\theta-\frac{1}{2}\eta\theta'\right),$$

then equation (4.29) becomes,

$$u\frac{\partial T}{\partial x} = \frac{abx}{(1-ct)^3}\theta f'$$

Multiplying equation (4.19) by $\frac{\nu(1-ct)}{a\alpha(T_w - T_\infty)}$, then

$$\frac{abx}{(1-ct)^3}\theta f'\frac{\nu(1-ct)}{a\alpha(T_w - T_\infty)} = \frac{bx}{(1-ct)^2}\frac{\nu}{\alpha}\theta f'\frac{1}{T_w - T_\infty}$$

$$= \frac{bx}{(1-ct)^2}\frac{\nu}{\alpha}\theta f'\frac{1}{T_w + \frac{bx}{(1-ct)^2} - T_\infty}$$

$$\frac{bx}{(1-ct)^2}\frac{\nu}{\alpha}\theta f'\frac{(1-ct)^2}{bx} = \frac{\nu}{\alpha}\theta f' = Pr\theta f'$$

equation (4.28) becomes,

$$-\frac{a}{1-ct}(T_w - T_\infty)f\theta'\frac{\nu(1-ct)}{a\alpha(T_w - T_\infty)} = -Prf\theta',$$

equation (4.29) becomes,

$$-\frac{1}{\rho C_p}\frac{16\sigma^* T_\infty^3}{3k^*}\frac{a}{\nu(1-ct)}(T_w - T_\infty)\theta''\frac{\nu(1-ct)}{a\alpha(T_w - T_\infty)} = -Nr\theta'',$$

where Nr is the radiation parameter.

equation (4.30) becomes,

$$\frac{a^3x^2}{\rho C_p(1-ct)^3}\left(f''\right)^2\frac{\nu(1-ct)}{a\alpha(T_w - T_\infty)} = \frac{a^2x^2}{(1-ct)^2}\frac{1}{C_p(T_w - T_\infty)}\frac{\nu}{\alpha}\left(f''\right)^2$$

$$= u^2\frac{1}{C_p(T_w - T_\infty)}Pr\left(f''\right)^2 = PrEc\left(f''\right)^2$$

equation (4.31) becomes,

$$\frac{a}{1-ct}Q(T_w - T_\infty)\theta\frac{\nu(1-ct)}{a\alpha(T_w - T_\infty)} = \frac{\nu}{\alpha}Q\theta' = PrQ\theta$$

Therefore, when combine all equations we get the following non-linear ordinary differential equation,

$$\theta'' + Nr\theta'' + Prf\theta' - Pr\theta f' + PrEc\left(f''\right)^2 + PrQ\theta - APr\left(2\theta + \frac{1}{2}\eta\theta'\right) = 0,$$

$$(1+Nr)\theta'' + Pr(f\theta' - f'\theta) + PrEc\left(f''\right)^2 + PrQ\theta - APr\left(2\theta + \frac{1}{2}\eta\theta'\right) = 0,$$

where $Nr = \frac{16\sigma^* T_\infty}{3kk^*}$ is the thermal radiation parameter.

4.1.4 Similarity transformation for Species concentration:

$$\frac{\partial C}{\partial t}+u\frac{\partial C}{\partial x}+v\frac{\partial C}{\partial y}=D\frac{\partial^2 C}{\partial y^2}-K(C-C_\infty),\qquad \phi=\frac{C-C_\infty}{C_w-C_\infty}$$

$$C-C_\infty=\phi(C_w-C_\infty)$$

$$C=\phi(C_w-C_\infty)+C_\infty$$

$$\frac{\partial C}{\partial t}=\frac{2mcx}{(1-ct)^3}\phi+\frac{\partial}{\partial t}\left(\phi(C_w-C_\infty)+C_\infty\right)$$

$$=\frac{2mcx}{(1-ct)^3}\phi+(C_w-C_\infty)\frac{\partial\phi}{\partial\eta}\frac{\partial\eta}{\partial t}$$

$$=\frac{2mcx}{(1-ct)^3}\phi+(C_w-C_\infty)\phi(-\frac{1}{2}\frac{\eta c}{1-ct})$$

$$\frac{\partial C}{\partial t}=\frac{2mcx}{(1-ct)^3}\phi-\frac{1}{2}\frac{\eta c}{1-ct}(C_w-C_\infty)\phi' \tag{4.33}$$

$$\frac{\partial C}{\partial x}=\frac{m}{(1-ct)^2}\phi$$

$$u\frac{\partial C}{\partial x}=\frac{a}{(1-ct)}xf'\frac{m}{(1-ct)^2}=\frac{amx}{(1-ct)^3}\phi f' \tag{4.34}$$

$$\frac{\partial C}{\partial y}=\frac{\partial}{\partial y}\left(\phi(C_w-C_\infty)+C_\infty\right)$$

$$=(C_w-C_\infty)\frac{\partial\phi}{\partial\eta}\frac{\partial\eta}{\partial y}=(C_w-C_\infty)\phi'\left(\frac{a}{\nu(1-ct)}\right)^{\frac{1}{2}}=\left(\frac{a}{\nu(1-ct)}\right)^{\frac{1}{2}}(C_w-C_\infty)\phi'$$

$$v\frac{\partial C}{\partial y}=-(C_w-C_\infty)\phi'\left(\frac{\nu a}{(1-ct)}\right)^{\frac{1}{2}}f\left(\frac{a}{\nu(1-ct)}\right)^{\frac{1}{2}}$$

$$v\frac{\partial C}{\partial y}=-\frac{a}{1-ct}(C_w-C_\infty)f\phi \tag{4.35}$$

$$\frac{\partial^2 C}{\partial y^2} = \frac{\partial}{\partial y}\left(\frac{\partial C}{\partial y}\right)$$

$$= \frac{\partial}{\partial y}\left(\frac{a}{\nu(1-ct)}\right)^{\frac{1}{2}}(C_w - C_\infty)\phi'$$

$$= (C_w - C_\infty)\frac{\partial \phi'}{\partial y}\frac{\partial \eta}{\partial y}\left(\frac{a}{\nu(1-ct)}\right)^{\frac{1}{2}}$$

$$= (C_w - C_\infty)\phi''\left(\frac{a}{\nu(1-ct)}\right)^{\frac{1}{2}}\left(\frac{a}{\nu(1-ct)}\right)^{\frac{1}{2}} = (C_w - C_\infty)\phi''\frac{a}{\nu(1-ct)}$$

$$= \frac{a}{\nu(1-ct)}(C_w - C_\infty)\phi''$$

$$D\frac{\partial^2 C}{\partial y^2} = \frac{a}{\nu(1-ct)}(C_w - C_\infty)\phi'' D \tag{4.36}$$

$$K(C - C_\infty) = K(C_w - C_\infty)\phi$$

$R = \frac{K(1-ct)}{a}$ is the local chemical reaction parameter

Make K the subject of the formula.

$$K = \frac{aR}{1-ct}$$

$$K(C - C_\infty) = \frac{a}{1-ct}R(C_w - C_\infty)\phi$$

$$\frac{\partial C}{\partial t} + u\frac{\partial C}{\partial x} + v\frac{\partial C}{\partial y} = D\frac{\partial^2 C}{\partial y^2} - K(C - C_\infty)$$

$$\frac{2mcx}{(1-ct)^3}\phi - \frac{1}{2}\frac{\eta c}{1-ct}(C_w - C_\infty)\phi' + \frac{amx}{(1-ct)^3}\phi f' - \frac{a}{1-ct}(C_w - C_\infty)f\phi'$$
$$= \frac{a}{\nu(1-ct)}D(C_w - C_\infty)\phi'' - \frac{a}{1-ct}R(C_w - C_\infty)\phi$$

$$\frac{\partial C}{\partial t} = \frac{2mcx}{(1-ct)^3}\phi - \frac{1}{2}\frac{\nu c}{1-ct}(C_w - C_\infty)\theta' \tag{4.37}$$

$$u\frac{\partial C}{\partial x} = 0 \tag{4.38}$$

$$v\frac{\partial C}{\partial y} = -\frac{a}{1-ct}(C_w - C_\infty)f\theta' \tag{4.39}$$

$$D\frac{\partial^2 C}{\partial y^2} = \frac{a}{\nu(1-ct)}(C_w - C_\infty)\phi'' D \tag{4.40}$$

$$K(C - C_\infty) = \frac{a}{1-ct}R(C_w - C_\infty)\phi \tag{4.41}$$

The purpose of the equations (4.37-4.41) is to combine all of them together to get the species concentration.

Multiply all equations from (4.37) to (4.41) by $\frac{\nu(1-ct)}{Da(C_w - C_\infty)}$

equation (4.37) becomes,

$$\frac{2mcx}{(1-ct)^3}\phi\frac{\nu(1-ct)}{Da(C_w - C_\infty)} - \frac{1}{2}\frac{\nu c}{1-ct}(C_w - C_\infty)\theta'\frac{\nu(1-ct)}{Da(C_w - C_\infty)} = -\frac{1}{2}\eta\frac{c}{a}\frac{\nu}{D}\phi'$$

$$= 2\frac{c}{a}\frac{\nu}{D}\phi - \frac{1}{2}\eta ASc\phi' = 2ASc\phi - \frac{1}{2}\eta ASc\phi' = ASc(2\phi - \frac{1}{2}\eta\phi')$$

where, $\frac{c}{a} = A$ is the unsteady parameter and $\frac{\nu}{D} = Sc$ is the Schmidt number

equation (4.37) becomes,

$$u\frac{\partial C}{\partial x} = \frac{amx}{(1-ct)^3}\phi f' = \frac{amx}{(1-ct)^3}\phi f'\frac{\nu(1-ct)}{Da(C_w - C_\infty)}$$

$$= \frac{mx}{(1-ct)^2}\frac{nu}{D}\frac{1}{(C_w - C_\infty)}\phi f' = \frac{mx}{(1-ct)^2}\frac{\nu}{D}\frac{1}{C_\infty + \frac{mx}{(1-ct)^2} - C_\infty}\phi f'$$

$$= \frac{mx}{(1-ct)^2}\frac{\nu}{D}\frac{(1-ct)^2}{mx}\phi f' = Sc\phi f'$$

equation (4.39) becomes,

$$-\frac{a}{1-ct}(C_w - C_\infty)f\theta'\frac{\nu(1-ct)}{Da(C_w - C_\infty)} = -\frac{\nu}{D}f\phi' = -Scf\phi'$$

equation (4.40) becomes,

$$\frac{a}{\nu(1-ct)}(C_w - C_\infty)\phi'' D\frac{\nu(1-ct)}{Da(C_w - C_\infty)} = \phi''$$

$$\frac{a}{1-ct}R(C_w - C_\infty)\phi\frac{\nu(1-ct)}{Da(C_w - C_\infty)} = \frac{\nu}{D}R\phi = ScR\phi$$

Therefore, we combine (4.37 to 4.41) equations we get the following non-linear ordinary differential equation,

$$\phi'' + Sc(f\phi' - f'\phi) - ASc\left(2\phi + \frac{1}{2}\eta\phi'\right) - KSc\phi = 0$$

Utilising the similar variables in equations (3.5), (3.27), (3.45) and (3.62) we derive the following system of ordinary differential equations,

$$f''' + f''f - Mf' - f'^2 - A\left(f' + \frac{1}{2}\eta f''\right) + \lambda(\theta + N\phi) = 0 \tag{4.42}$$

$$(1+Nr)\theta'' + Pr(f\theta' - f'\theta) + PrEc\left(f''\right)^2 + PrQ\theta - APr\left(2\theta + \frac{1}{2}\eta\theta'\right) = 0 \tag{4.43}$$

$$\phi'' + Sc(f\phi' - f'\phi) - ASc\left(2\phi + \frac{1}{2}\eta\phi'\right) - KSc\phi = 0 \tag{4.44}$$

4.2 Similarity transformation for boundary conditions

Equation (3.63) and (3.64) are boundary conditions, now the transformed boundary conditions are,

Case 1, At $y = 0$, where $s = \frac{-V_w}{\sqrt{\frac{1-ct}{\nu a}}}$

Therefore, $V_w = -\sqrt{\frac{1-ct}{\nu a}}s$

$$\begin{aligned}
&u = U_w = \tfrac{ax}{1-ct}f'(0) = \tfrac{ax}{1-ct} = f'(0) = 1\\
&v = V_w = -\left(\tfrac{\nu a}{1-ct}\right)^{\frac{1}{2}}f(0) = V_w = -\sqrt{\tfrac{\nu a}{1-ct}}f(0) = -\sqrt{\tfrac{1-ct}{\nu a}}s = f(0) = s\\
&T = T_w = \theta(T_w - T_\infty) + T_\infty = T_\infty + \tfrac{bx}{(1-ct)^2} = \theta\left(T_\infty + \tfrac{bx}{(1-ct)^2} - T_\infty\right) + T_\infty\\
&= T_\infty + \tfrac{bx}{(1-ct)^2} = \theta\tfrac{bx}{(1-ct)^2} = \tfrac{bx}{(1-ct)^2} = \theta(0) = 1\\
&C = C_w = \phi(C_w - C_\infty) + C_\infty = C_\infty + \tfrac{mx}{(1-ct)^2} = \phi\left(C_\infty + \tfrac{mx}{(1-ct)^2} - C_\infty\right) + C_\infty\\
&= C_\infty + \tfrac{mx}{(1-ct)^2} = \phi\tfrac{mx}{(1-ct)^2} = \tfrac{mx}{(1-ct)^2} = \phi(0) = 1
\end{aligned} \tag{4.45}$$

Therefore,

$$f'(0) = 1, \quad f(0) = s, \quad \theta(0) = 1, \quad \phi(0) = 1$$

Case 2, At $y \longrightarrow \infty$

$$\begin{aligned} &u \longrightarrow 0 = \tfrac{ax}{1-ct} f'(\infty) \longrightarrow 0 = f'(\infty) \longrightarrow 0 \\ &T \longrightarrow T_\infty = \theta(T_w - T_\infty) + T_\infty \longrightarrow T_\infty = \theta(T_w - T_\infty) \longrightarrow 0 = \theta(\infty) \longrightarrow 0 \\ &C \longrightarrow C_\infty = \phi(C_w - C_\infty) + C_\infty \longrightarrow C_\infty = \phi(C_w - C_\infty) \longrightarrow 0 = \phi(\infty) \longrightarrow 0 \end{aligned} \tag{4.46}$$

Therefore,

$$f'(\infty) \longrightarrow 0, \quad \theta(\infty) \longrightarrow 0, \quad \phi(\infty) \longrightarrow 0$$

where u and v are velocity components in x and y direction, U_w is the stretching sheet wall velocity, a, b, c and m are constants, f is the dimensionless stream function, θ is the dimensionless temperature and ϕ is the dimensionless species concentration.

4.3 The important physical parameters

In this study, we have the following significant physical parameters, that is, the friction of the skin C_f, the local Nusselt number Nu_x and the local Sherwood number Sh_x.. From the engineering frame of reference, the physical quantities of significance are the local Skin-friction, the local Nusselt number and the local Sherwood number which are defined in Mitiku et. al [20].

4.3.1 The Skin-friction

$$C_f = \frac{2\tau_w}{\rho u_w^2} \tag{4.47}$$

where τ_w is the surface shear stress, $\tau_w =$ $\tau_w = \mu \frac{\partial u}{\partial y} \Big|_{y=0}$

$$\tau_w = \mu \frac{\partial}{\partial y} \left(\frac{ax}{1-ct} f'(0) \right) \frac{\partial \eta}{\partial y}$$

$$\tau_w = \mu \frac{ax}{1-ct} f''(0) \sqrt{\frac{a}{\nu(1-ct)}}$$

We know that $u_w = \frac{ax}{1-ct}$ therefore,

$$\tau_w = \mu u_w f''(0) \sqrt{\frac{a}{\nu(1-ct)}} \tag{4.48}$$

Substituting equation (4.48) into equation (4.47) we get

$$C_f = \left(2\mu u_w f''(0) \sqrt{\frac{a}{\nu(1-ct)}} \right) \div \rho u_w^2$$

$$C_f = \left(2\mu u_w f''(0) \sqrt{\frac{a}{\nu(1-ct)}} \right) \frac{1}{\rho u_w^2}$$

$$\frac{1}{2} C_f \frac{\rho}{\mu} \frac{u_w}{\sqrt{\frac{a}{\nu(1-ct)}}} = f''(0) \tag{4.49}$$

4.3.2 The local Nusselt number:

$$Nu_x = \frac{xq_w}{k(T_w - T_\infty)} \tag{4.50}$$

where q_w is the wall heat flux, $q_w = \quad q_w = -k\frac{\partial T}{\partial y}\Big|_{y=0}$

$$q_w = \frac{-kbx}{(1-ct)^2}\theta'(0)\frac{\partial \eta}{\partial y}$$

$$q_w = \frac{-kbx}{(1-ct)^2}\theta'(0)\sqrt{\frac{a}{\nu(1-ct)}} \tag{4.51}$$

Substituting equation (4.51) into equation (4.50) we get

$$Nu_x = \left(x\frac{-kbx}{(1-ct)^2}\theta'(0)\sqrt{\frac{a}{\nu(1-ct)}}\right) \div k(T_w - T_\infty)$$

$$Nu_x = \left(x\frac{-kbx}{(1-ct)^2}\theta'(0)\sqrt{\frac{a}{\nu(1-ct)}}\right) \div k\left[T_\infty + \frac{bx}{(1-ct)^2} - T_\infty\right]$$

$$Nu_x = \left(x\frac{-kbx}{(1-ct)^2}\theta'(0)\sqrt{\frac{a}{\nu(1-ct)}}\right) \div \frac{kbx}{(1-ct)^2}$$

$$Nu_x = \left(x\frac{-kbx}{(1-ct)^2}\theta'(0)\sqrt{\frac{a}{\nu(1-ct)}}\right) \frac{(1-ct)^2}{kbx}$$

$$Nu_x = -x\theta'(0)\sqrt{\frac{a}{\nu(1-ct)}}$$

So we get

$$\frac{Nu_x}{x\sqrt{\frac{a}{\nu(1-ct)}}} = -\theta'(0) \tag{4.52}$$

4.3.3 The local Sherwood number:

$$Sh_x = \frac{xq_m}{D(C_w - C_\infty)} \tag{4.53}$$

where q_m is the mass flux, $q_m = \quad q_m = -D\frac{\partial C}{\partial y}\Big|_{y=0}$

$$q_m = \frac{-Dmx}{(1-ct)^2}\phi\frac{\partial \eta}{\partial y}$$

$$q_m = \frac{-Dmx}{(1-ct)^2}\phi'(0)\sqrt{\frac{a}{\nu(1-ct)}} \tag{4.54}$$

Substituting equation (4.54) into equation (4.53) we get

$$Sh_x = \left(x\frac{-Dmx}{(1-ct)^2}\phi'(0)\sqrt{\frac{a}{\nu(1-ct)}}\right) \div D(C_w - C_\infty)$$

$$Sh_x = \left(x\frac{-Dmx}{(1-ct)^2}\phi'(0)\sqrt{\frac{a}{\nu(1-ct)}}\right) \div D\left[C_\infty + \frac{bx}{(1-ct)^2} - C_\infty\right]$$

$$Sh_x = \left(x\frac{-Dmx}{(1-ct)^2}\phi'(0)\sqrt{\frac{a}{\nu(1-ct)}}\right) \div \frac{Dmx}{(1-ct)^2}$$

$$Sh_x = \left(x\frac{-Dmx}{(1-ct)^2}\phi'(0)\sqrt{\frac{a}{\nu(1-ct)}}\right) \frac{(1-ct)^2}{Dmx}$$

$$Sh_x = -x\phi'(0)\sqrt{\frac{a}{\nu(1-ct)}}$$

So we get

$$\frac{Sh_x}{x\sqrt{\frac{a}{\nu(1-ct)}}} = -\phi'(0) \tag{4.55}$$

Chapter 5

Method of the solution

In this chapter, we give the definition of a general overview of the implementation of the SRM iterative scheme for the present non-linear coupled system of differential equations and brief about how to test the convergence of Spectral Relaxation Method (SRM).

5.1 Boundary value problems

The Boundary Value Problems are a systems of ordinary differential equations which have a solution and derivative values detailed at more than one point. Most frequently, the solution and derivatives are specified at just two points (the boundary) defining boundary value problems. Boundary Value Problems are complex to model, therefore, it is crucial to transform them from partial to ordinary differential eqaution, then these ordinary differential equations are solved numerically using techniques such as Runge-Kutta, Matlab BVP method among others.

5.2 The SRM and implementation of SRM

The Spectral Relaxation Method (SRM) is a numerical and computer-based technique of deciphering a variability of practical engineering problems that arises in different fields such as, in heat transfer, fluid mechanics. It is recognized by developers and users as one of the most powerful numerical analysis tools ever devised to analyze multifaceted problems in engineering. The sophistication of the method is its accuracy, simplicity, and

computability all make it extensively used a tool in the engineering modelling and design process. It has been useful to a number of physical problems, where the governing differential equations are elucidated by transforming them into unassuming iteration schemes.

The SRM scheme simply involves rearranging the governing equations in a particular order, starting with the one that has the least number of unknown functions. After we employ the Gauss-Seidel method for purpose of decoupling the system. Regularly, the Gauss-Seidel is used to decouple linear systems of algebraic equations. Then we linearise the system without using Taylor expansions or any such method. All these three steps break down the non-linear coupled system into a sequence of linear decoupled subsystems that are easily solved. The following steps involved in developing the SRM iterative scheme [22]:

5.3 Algorithm

1. Rewrite the equations in some chronological order, starting with the one that has the least number of unknowns.

2. Starting with the first equation, determine the unknown variable with the highest order in each equation. Replace these unknowns with some unique Z_i; where $i = 1, 2, 3, ..., m$ and m is the total number of non-linear equations. This is such that the unknown associated with the highest order in equations $1, 2, 3, ..., m$ is marked as $Z_1, Z_2, Z_3, ..., Z_m$, respectively.

3. For the first equation ($i = 1$), the linear terms in Z_1 are estimated at the present iteration and hence they are discretized as $Z_{1,r+1}$. The other unknowns $(Z_2, Z_3, ..., Z_m)$ appearing in equation 1 are assumed to be computed in the previous iteration and hence they are labelled as $Z_{i,r}$ where $i = 2, 3, ..., m$. This facilitates decoupling of the equation. On the same equation, we assume that the non-linear terms in Z_1 are pre-determined

and so they are denoted by $r(i.e.Z_{1,r})$. This serves the purpose of linearizing without the application of Taylor expansion or any other linearizing method.

4. On the second equation $(i = 2)$ the linear terms in Z_2 are denoted by $r + 1$ since they are evaluated at the current iteration. The recently computed solution of Z_1 in equation 1 is used immediately here and hence each Z_1 must be subscripted as $Z_{1,r+1}$. This is how the scheme resembles the Gause Seidel method. The other unknown appearing in equation Z are assumed to be computed from the previous iteration and hence they are labelled as $Z_{i,r}$, where $i = 3, 4, ..., m$. We assume that the non-linear terms in Z_2 are pre-determined and so they are discretised by $r(i.e.Z_{2,r})$. This serves the purpose of linearizing.

5. For $i = 3$, the linear terms of Z_3 are denoted by $r + 1$ since they are evaluated at the current iteration. The recently computed solutions of Z_1 and Z_2 in equation 1 and 2, respectively are used immediately. As a result, Z_1 and Z_2 are denoted by $r + 1$. All the other terms in $Z_3, Z_4, ..., Z_m$ are assumed to be pre-determined and hence they are discretised by r.

6. We carry on this process in all the remaining equations. For the last equation, $i = m$, the linear terms in Z_m are discretised as $Z_{m,r+1}$. The non-linear terms in Z_m are denoted by r. All the other terms (linear or non-linear) involving $Z_1, Z_2, Z_3, ..., Z_{m+1}$ are discretised by $r+1$ since they are known from the previous equations. The same iterative scheme is described by Motsa [21] as follows:

Consider a system of m non-linear ordinary differential equations with m unknown functions
$Z_i(\omega)(i = 1, 2, ..., m)$ where ω is the independent variable in the region [0,1]. We construct the vector Z_i whose elements are all the derivatives of the variable Z_i with respect to ω. The vector is given as follows,

$$[H]Z_i(\omega) = \left[Z_i^0, Z_i^1, ..., Z_i^{n_i}\right],$$

where $Z_i^0 = Z_i, Z_i^p$ is the pth derivative of Z_i with respect to ω and $Z_i^{n_i} (i = 1, 2, ..., m)$ is the highest order derivative of the variable Z_i in the system of equations.
Each $Z_{i^{th}}$ equation in the system can be written in the form,

$$\pounds_i [Z_1, Z_2, ..., Z_m] = N_i [Z_1, Z_2, ..., Z_m] + H_i(\omega), i = 1, 2, ..., m \tag{5.1}$$

where $\pounds_i$ and N_i are linear and non-linear operators respectively. $H(\omega)$ is a known function in ω. If we let r and $r + 1$ denote the previous and current iterations then each N_i can be linearised as follows,

$$N_i [Z_1, Z_2, ..., Z_m] = N_i [Z_1, Z_2, ..., Z_{i,r}, Z_{i+1}, ..., Z_{m-1}, Z_m] \tag{5.2}$$

Applying the Gauss Seidel approach on the resultant non-linear system we develop the SRM iterative scheme as follows,

$$\pounds_1 [Z_{1,r+1}, Z_{2,r}, ..., Z_{m-1,r}, Z_{m,r}] = N_1 [Z_{1,r}, Z_{2,r}, ..., Z_{m,r}] + H_1(\omega),$$

$$\pounds_2 [Z_{1,r+1}, Z_{2,r+1}, Z_{3,r}....., Z_{m,r}] = N_2 [Z_{1,r+1}, Z_{2,r}, Z_{3,r}....., Z_{m,r}] + H_2(\omega),$$

$$\pounds_3 [Z_{1,r+1}, Z_{2,r+2}, Z_{3,r+1}, Z_{4,r}....., Z_{m,r}] = N_3 [Z_{1,r+1}, Z_{2,r+1}, Z_{3,r}....., Z_{m,r}] + H_3(\omega),$$

$$\pounds_i [Z_{1,r+1}, Z_{i,r+1}, Z_{i+1,r}....., Z_{m,r}] = N_i [Z_{i,r+1}, Z_{2,r+1}, Z_{i-1,r+1}, Z_{i,r}....., Z_{m,r}] + H_i(\omega) \tag{5.3}$$

Therefore, starting from the initial approximation $Z_{1,0}, Z_{2,0}, Z_{3,0}, ..., Z_{m,0}$ the SRM iterative scheme (5.3) can be repeatedly solved until the desired level of accuracy is reached for all the unknown $(Z_1, Z_2, ..., Z_m)$.

The Spectral relaxation Method (SRM) is a proposed new algorithm for the solution of boundary value problems of the form (4.32)-(4.36). The algorithm follows the idea of the Gauss-Seidel method. Hence, an iteration scheme is developed by evaluating linear terms in the current iteration level (denoted by $r + 1$) and all other terms (linear and non-linear) in the previous iteration level (denoted by r). The decoupled equation system is solved using the Chebyshev pseudo spectral method (cite9, cite21). The basic thought

behind the spectral collocation method is the first appearance of a differentiation matrix D which is applied to approximate the differential coefficient of the unknown variables, for instance, $f(eta)$ at the collocation points is represented as the matrix vector product.

$$\frac{df}{d\eta} = \sum_{k=0}^{\bar{N}} D_{lk} f(\tau_k) = Df, l = 0, 1....., \bar{N} \tag{5.4}$$

where $\bar{N} + 1$ is the number of collocation points (grid points),

$$D = \frac{2D}{\eta_\infty}, \tag{5.5}$$

and

$$f = \left[f(\tau_0), f(\tau_1), f(\tau\bar{N})\right]^T \tag{5.6}$$

Equation (5.4) is the vector function at the collocation points. Higher order derivatives are obtained as powers of D, that is,

$$f^g = D^g Z, \tag{5.7}$$

where g is the order of the derivatives, $eta_i nfty$ is a finite length that is chosen to be numerically large enough to approximate the conditions at infinity in the governing problems and the stress tensor tau is a variable used to map the truncated interval $[0, eta]$ to the interval $[-1, 1]$ on which the spectral method can be implemented.

5.3.1 Application of SRM

The application of spectral relaxation technique to (4.31)-(4.35), enhance the production of following iteration method, first, we set $f'(\eta) = g(\eta)$ and deduce the following iteration scheme.

$$g'' + fg' - Mg - g^2 - A(g + \frac{1}{2}\eta g') + \lambda(\theta + N\phi) = 0 \tag{5.8}$$

We set L_2 be the terms of g derivatives and N_2 be terms independent of g derivatives.

$$L_2 = g'' + fg' - Mg - A(g + \frac{1}{2}\eta g') \tag{5.9}$$

$$N_2 = -g^2 + \lambda(\theta + N\phi) \tag{5.10}$$

$$H_2 = 0 \tag{5.11}$$

$$L_2|_{r+1} = g''_{r+1} + fg'_{r+1} - Mg_{r+1} - A(g_{r+1} + \frac{\eta}{2}g'_{r+1}) \tag{5.12}$$

$$N_2|_r = -g_r^2 + \lambda(\theta + N\phi) \tag{5.13}$$

Therefore,

$$L_2 = N_2 + H_2 \tag{5.14}$$

$$g''_{r+1} + f_{r+1}g'_{r+1} - Mg_{r+1} - Ag_{r+1} - \frac{\eta}{2}g'_{r+1} = g_r^2 - \lambda(\theta_r + N\phi_r)$$

$$g''_{r+1} + \left(f_{r+1} - \frac{\eta}{2}\right)g'_{r+1} - (M + A)g_{r+1} = g_r^2 - \lambda(\theta_r + N\phi_r) \tag{5.15}$$

$$(1 + N_r)\theta'' + Pr(f\theta' - g\theta) + PrEc(g')^2 + PrQ\theta - APr\left(2\theta + \frac{\eta}{2}\theta'\right) \tag{5.16}$$

$$L_3 = (1 + Nr)\theta'' + Pr(f\theta' - g\theta) + PrQ\theta - APr\left(2\theta + \frac{\eta}{2}\theta'\right) \tag{5.17}$$

$$N_3 = -PrEc(g')^2 \tag{5.18}$$

$$H_3 = 0 \tag{5.19}$$

$$L_3|_{r+1} = (1 + Nr)\theta''_{r+1} + Pr(f_{r+1}\theta'_{r+1} - g_{r+1}\theta_{r+1}) + PrQ\theta_{r+1} - APr\left(2\theta_{r+1} + \frac{\eta}{2}\theta'_{r+1}\right) \tag{5.20}$$

$$N_3|_r = -PrEc(g'_{r+1})^2 \tag{5.21}$$

Therefore,

$$L_3 = N_3 + H_3 \tag{5.22}$$

$$(1+Nr)\theta''_{r+1}+\left(f_{r+1}-A\frac{\eta}{2}\right)Pr\theta'_{r+1}+(Q-g_{r+1}+2A)\,Pr\theta_{r+1}=-PrEc(g'_{r+1})^2 \quad (5.23)$$

$$\phi''+Sc(f\phi'-g\phi)-ASc\left(2\phi+\frac{\eta}{2}\phi'\right)-RSc\phi=0 \quad (5.24)$$

$$L_4=\phi''+Sc(f\phi'-g\phi)-ASc\left(2\phi+\frac{\eta}{2}\phi'\right)-RSc\phi \quad (5.25)$$

$$N_4=0, H_4=0 \quad (5.26)$$

$$L_4|_{r+1}=\phi''_{r+1}+Sc(f_{r+1}\phi'_{r+1}-g_{r+1}\phi_{r+1})-ASc\left(2\phi_{r+1}+\frac{\eta}{2}\phi'_{r+1}\right)-KSc\phi_{r+1} \quad (5.27)$$

Therefore,

$$L_4=N_4+H_4 \quad (5.28)$$

$$\phi''_{r+1}+Sc(f_{r+1}\phi'_{r+1}-g_{r+1}\phi_{r+1})-ASc\left(2\phi_{r+1}+\frac{\eta}{2}\phi'_{r+1}\right)-KSc\phi_{r+1}=0 \quad (5.29)$$

$$\phi''_{r+1}+Scf_{r+1}\phi'_{r+1}-Scg_{r+1}\phi_{r+1}-2ASc\phi_{r+1}-ASc\frac{\eta}{2}\phi'_{r+1}-KSc\phi_{r+1}=0$$

$$\phi''_{r+1}+\left(f_{r+1}-A\frac{\eta}{2}\right)Sc\phi'_{r+1}-(g_{r+1}+2A+K)Sc\phi_{r+1}=0 \quad (5.30)$$

So applying the spectral relaxation method on the resulting system of non-linear partial differential equations gives the following linear ordinary differential equations,

$$g''_{r+1}+\left(f-\frac{\eta}{2}\right)g'_{r+1}-(M+A)g_{r+1}=g_r^2-\lambda\theta_r-\lambda N\phi_r \quad (5.31)$$

$$\frac{(1+Nr)}{Pr}\theta''_{r+1}+\left(f_{r+1}-A\frac{\eta}{2}\right)\theta'_{r+1}+(Q-g_{r+1}+2A)\,\theta_{r+1}=-Ec(g'_{r+1})^2 \quad (5.32)$$

$$\phi''_{r+1}+\left(f_{r+1}-A\frac{\eta}{2}\right)Sc\phi'_{r+1}-(g_{r+1}+2A+K)Sc\phi_{r+1}=0 \quad (5.33)$$

With the following boundary conditions,

$$\begin{aligned} &f_{r+1}(0)=s, \quad g(0)=1, \quad \theta_{r+1}(0)=1, \quad \phi_{r+1}(0)=1 \quad \text{at} \quad \eta=0 \\ &g_{r+1}(\infty)=0, \quad \theta_{r+1}(\infty)=0, \quad \phi_{r+1}(\infty)=0 \quad \text{at} \quad \eta\longrightarrow\infty \end{aligned} \quad (5.34)$$

5.3.2 Applying the Chebyshev pseudo-spectral method

Now we apply the chebyshev pseudo-spectral method on (5.31)-(5.34), we obtain the following,

$$\begin{pmatrix} A_{11} & A_{12} & A_{13} \\ 0 & A_{22} & 0 \\ 0 & 0 & A_{33} \end{pmatrix} \begin{pmatrix} g_{r+1} \\ \theta_{r+1} \\ \phi_{r+1} \end{pmatrix} = \begin{pmatrix} B_1 \\ B_2 \\ B_3 \end{pmatrix}$$

$$\begin{aligned} &A_{11}g_{r+1} + A_{12}\theta_{r+1} + A_{13}\phi_{r+1} = B_1 \\ &A_{21}g_{r+1}A_{22}\theta_{r+1} = B_2 \\ &A_{31}g_{r+1} + A_{33}\phi_{r+1} = B_3 \end{aligned} \tag{5.35}$$

where

$$\begin{aligned} &A_{11} = D_2 + diag\left[f_{r+1} - \tfrac{\eta}{2}\right] D - (M + A)I, \\ &A_{12} = -\lambda I, \\ &A_{13} = -\lambda N I, \\ &B_1 = g_r^2 \\ &A_{22} = (1 + Nr)D_2 + diag\left[Pr\left(f_{r+1} - A\tfrac{\eta}{2}\right)\right] D - diag(Prg_r) + (Q - 2A)PrI, \\ &B_2 = -PrEc(g'_{r+1})^2 \\ &A_{33} = D_2 + diag\left[Sc\left(f_{r+1} - A\tfrac{\eta}{2}\right)\right] D - diag(Scg_r) - (2A + K)ScI, \\ &B_3 = 0 \end{aligned} \tag{5.36}$$

The boundary conditions are,

$$\begin{aligned} &f_{r+1}(\tau\bar{N}) = s \\ &g_{r+1}(\tau\bar{N}) = 1, g_{r+1}(\tau 0) = 0 \\ &\theta_{r+1}(\tau\bar{N}) = 1, \theta_{r+1}(\tau 0) = 0 \\ &\phi_{r+1}(\tau\bar{N}) = 1, \phi_{r+1}(\tau 0) = 0 \end{aligned} \tag{5.37}$$

In equations (5.36)-(5.37), I is an identity matrix of size $(\bar{N}+1) \times (\bar{N}+1)$, and diag[] is a diagonal matrix, all size $(\bar{N}+1) \times (\bar{N}+1)$ where $\bar{N}$ is the number of grid points, f, θ

and ϕ are the values of functions f, θ and ϕ, respectively, evaluated at the grid points. Equation (5.36) represents the Spectral relaxation method (SRM) scheme.

To compute the initial guess we use the following boundary conditions,

$$f(0) = s, \quad f'(0) = 1, \quad \theta(0) = 1, \quad \phi(0) = 0, \quad f'(\infty) \to 0, \quad \theta(\infty) \to 0, \quad \phi(\infty) \to 0, \quad \eta \to \infty$$

The initial guesses to start the SRM scheme for equations (5.31)-(5.33) are chosen as functions that satisfy the boundary conditions. From physical considerations, the velocity and temperature profiles for the boundary layer problem discussed in this work decay exponentially at $\eta = \infty$. For this reason, it is convenient to choose the following exponential functions as an initial guess,

$$\theta_0(\eta) = Ae^{-\eta} \tag{5.38}$$

When $\theta(0) = 1$, we get, $A = 1$, therefore,

$$\theta_0(\eta) = e^{-\eta} \tag{5.39}$$

$$\phi_0(\eta) = Ae^{-\eta} \tag{5.40}$$

When $\phi(0) = 1$, we get, $A = 1$, therefore,

$$\phi_0(\eta) = e^{-\eta} \tag{5.41}$$

$$f = a + b\eta + ce^{-\eta} \tag{5.42}$$

$$f' = b - ce^{-\eta} \tag{5.43}$$

When $f'(0) = 1$, we get,

$$1 = b - c$$

$$c = -1 + b \tag{5.44}$$

When $f = s$ and $\eta = 0$ we get,

$$s = a + b(0) + ce^{-0}$$

$$s = a + c \tag{5.45}$$

Substituting c into (5.45) we get,

$$s = a - 1 + b$$

Therefore,

$$a = s + 1 - b \tag{5.46}$$

Now substituting a and c into (5.42) we get,

$$f = s + 1 - b + b\eta + (-1 + b)e^{-\eta}$$

$$f = s + 1 - b + b\eta - e^{-\eta} + be^{-\eta} \tag{5.47}$$

When $f' \to \infty$, we get,

$$f'(\infty) = b - ce^{-\infty}$$

$$f'(\infty) = b \tag{5.48}$$

$$b = 0$$

Therefore,

$$f = s + 1 - e^{-\eta} \tag{5.49}$$

The initial guess are,

$$\theta_0(\eta) = e^{-\eta}, \quad \phi_0(\eta) = e^{-\eta}, \quad f_0(\eta) = s + 1 - e^{-\eta} \tag{5.50}$$

5.3.3 Test for convergence

To analyse the convergence of the iterative scheme we consider the error due to decoupling (E_d) of the unknown functions for each $(r+1)^{th}$ iteration. E_d is basically the infinity norm of the solutions of each unknown between two successive iterations. That is,

$$E_d = Max\left(\| Z_{1,r+1} - Z_{1,r+} \|_\infty, \| Z_{2,r+1} - Z_{2,r} \|_\infty, ..., \| Z_{m,r+1} - Z_{m,r} \|_\infty\right) \quad (5.51)$$

where $Z_i, i = 1, 2, ..., N$ where N is the total number of iteration. Then the iterative scheme is said to be convergent if,

$$e_1 > e_2 > e_3 > ..... > e_N \quad (5.52)$$

This is to say that the iterative scheme is convergent if E_d is inversely proportional to the number of iterations.

Chapter 6

Discussion of Results

The unstable hydromagnetic chemically transmitting assorted convection MHD fluid flow through a permeable stretching sheet embedded in a porous medium with thermal radiation and heat source has been investigated exploiting the Spectral Relaxation Method (SRM).

We start the discussion by outlining the result of the numerical calculations, the dimensionless velocity, temperature and species concentration distributions for the fluid flow under consideration. Their behaviour has been discussed for variations in the modelling parameters. The number of collocation point used in the SRM discretization is $N = 120$ in all cases. In this study, an efficient numerical method called Spectral Relaxation Method (SRM) has been used to solve the transformed equations (4.44) - (4.46) with the boundary conditions (4.45) and (4.46). In this study, we examined the effect of governing parameters on the transient velocity profile, temperature profile as well as the concentration profile. For purpose of discussing our results, the Spectral Relaxation Method (SRM) approach has been applied for various values of fluid flow controlling parameters, $Pr = 0.71, Sc = 0.62, A = 0.5, \lambda = 0.5, K = 0.5, N = 0.5, s = 0.5, Ec = 0.25, Nr = 0.5, M = 0.5, Q = 0.7$ to obtain a clear insight into the physics of the problem. The numerical values of the local Skin friction, the local Nusselt number and the local Sherwood number which are $f''(0), -\theta'(0), -\phi'(0)$, respectively are presented in tabular form.

For the purpose of accuracy and validation of the proposed method, we compare the results presented here and those obtained using the Matlab bvp4c scheme.

In the table 6.1, we compared two different techniques which are SRM and bvp4c by alternating the values of the unsteady parameter A. One discovers that the results are satisfactory and acceptable, we also determined that the time for SRM is very less compared to the bvp4c scheme. We conclude that the SRM is the best technique due to its accurate results, moreover, it is computationally efficient.

Table 6.1: Comparison of SRM and bvp4c with different values of A

			SRM		**bvp4c**
A	Iteration	Time(sec)	$f''(0)$	Time(S)	$f''(0)$
1	11	0.03	1.44886391	318.78	1.44886391
3	9	0.02	1.98273229	91.38	1.98273229
5	7	0.02	2.38336537	107.87	2.38336537
7	7	0.02	2.71996851	79.19	2.71996851

Table 6.2, shows the effects of various values of unsteady parameter on the local Skin friction coefficient $f''(0)$, local Nusselt number $-\theta'(0)$ and local Sherwood number $-\phi'(0)$ are shown in Table 6.2. From Table 6.2, one notices that as unsteady parameter (A) increase, the local Skin friction coefficient $f''(0)$, local Nusselt number $-\theta'(0)$ and local Sherwood number $-\phi'(0)$ increase.

Table 6.2: Effect of the unsteady parameter A on the $f''(0)$, $-\theta'(0)$ and $-\phi'(0)$

A	Time(sec)	$f''(0)$	$-\theta'(0)$	-$\phi'(0)$
0.5	0.03	1.25830852	0.75118722	1.38706369
0.8	0.03	1.37878360	0.92226582	1.50930767
1.0	0.03	1.44886391	1.01611382	1.58617363
1.5	0.05	1.60446209	1.21381891	1.76366480

Table 6.3 gives account on the effect of the Prandtl number on the local Skin friction, local Nusselt number, and the local Sherwood number. From Table 6.3, It is observed that as the Prandtl number (Pr) increases the local Skin friction $f''(0)$ local Nusselt number $-\theta'(0)$ increases while the local Sherwood number $-\phi'(0)$ decreases.

Table 6.3: Influence of the Prandtl number Pr on the $f''(0)$, $-\theta'(0)$ and $-\phi'(0)$

Pr	Time(sec)	$f''(0)$	$-\theta'(0)$	-$\phi'(0)$
0.7	0.04	1.25725486	0.74446149	1.38721761
0.9	0.04	1.27637057	0.87391231	1.38445335
1.5	0.04	1.31717901	1.21807547	1.37880055

Table 6.4 Shows the effects of the Schmidt number Sc on the local Skin friction $f''(0)$, local Nusselt number $-\theta'(0)$ and local Sherwood number $-\phi'(0)$. The Nusselt number $-\theta'(0)$ is decreased as the value of the Schmidt number Sc increases, while the local Skin friction and local Sherwood number increases.

Table 6.4: Effects of the Schmidt number Sc on the $f''(0)$, $-\theta'(0)$ and $-\phi'(0)$

Sc	Time(sec)	$f''(0)$	$-\theta'(0)$	-$\phi'(0)$
0.6	0.04	1.25726519	0.75154091	1.36020806
1.0	0.05	1.27331127	0.74658585	1.85010898
2.0	0.06	1.29351655	0.74179923	2.84360906

Table 6.5 shows the effects of the buoyancy parameter due to temperature λ on the local Skin friction, local Nusselt number and local Sherwood number. It can be seen that local Skin friction $f''(0)$ decreases as buoyancy parameter due to temperature (λ) increases, while local Nusselt number $-\theta'(0)$ and the local Sherwood number $-\phi'(0)$ increases. In

Table 6.5: Influence of the buoyancy parameter due to temperature λ on the $f''(0)$, $-\theta'(0)$ and $-\phi'(0)$

λ	Time(sec)	$f''(0)$	$-\theta'(0)$	-$\phi'(0)$
0	0.06	1.63017956	0.65646340	2.80854083
0.7	0.06	1.16919073	0.76658114	2.85564646
1	0.06	0.98977827	0.79821696	2.87235959

the table 6.6, it is shown the effects of the Eckert number Ec on the local Skin friction, local Nusselt number, and local Sherwood number. It is observed that as the Eckert number Ec increases the local Skin friction $f''(0)$ and the local Nusselt number $-\theta'(0)$ decreases while the local Sherwood number $-\phi'(0)$ increases.

Table 6.6: Effects of the Eckert number Ec on the $f''(0)$, $-\theta'(0)$ and $-\phi'(0)$

Ec	Time(sec)	$f''(0)$	$-\theta'(0)$	-$\phi'(0)$
1.0	0.08	1.28166844	0.57088983	2.84520464
3.0	0.08	1.25206894	0.14454105	2.84917178
3.5	0.07	1.24507190	0.04401958	2.85010588

Table 6.7, depicts the effect of magnetic parameter (M) on the local Skin friction $f''(0)$, local Nusselt number $-\theta''(0)$ and the local Sherwood number $-\phi''(0)$. The rate of Nusselt number $-\theta''(0)$ and the rate of Sherwood number $-\phi''(0)$ on the surface as expected are decreased as the magnetic parameter increases, while the rate of Skin friction $f''(0)$ increases as magnetic parameter increases.

Table 6.7: Effect of the magnetic parameter M on the $f''(0)$, $-\theta'(0)$ and $-\phi'(0)$

M	Time(sec)	$f''(0)$	$-\theta'(0)$	-$\phi'(0)$
0	0.03	1.03287771	0.79533811	1.40446386
0.5	0.03	1.25830852	0.75118722	1.38706369
2.5	0.02	1.93032658	0.63290654	1.34229646

In Table 6.8 we depict the effect of the local chemical reaction (K) on the local Skin friction $f''(0)$, local Nusselt number $-\theta(0)$, and local Sherwood number $-\phi''(0)$. We noticed that both local Skin friction and local Sherwood number are decreased with increasing values of the local chemical reaction (K) while the local Nusselt number increases as chemical reaction increasing.

Table 6.8: Effect of the chemical reaction K on the $f''(0)$, $-\theta'(0)$ and $-\phi'(0)$

K	Time(sec)	$f''(0)$	$-\theta'(0)$	-$\phi'(0)$
1.0	0.04	1.26308341	0.74959222	1.51382159
0.7	0.03	1.26035350	0.75049005	1.43949971
0.0	0.03	1.25207613	0.75345012	1.24265618

Table 6.9 shows the effect of the local heat source (Q) on the local Skin friction, local Nusselt number, and local Sherwood number. We noticed that both local Skin friction and local Nusselt number increases as the local heat source (Q) increases, while the local Sherwood number decreases as the local heat source (Q) increases.

Table 6.9: Effect of the local heat source/sink Q on the $f''(0)$, $-\theta'(0)$ and $-\phi'(0)$

Q	Time(sec)	$f''(0)$	$-\theta'(0)$	-$\phi'(0)$
0.5	0.04	1.27170885	0.8297709	1.38504540
0.3	0.03	1.28210794	0.89703998	1.38351731
0.0	0.03	1.29442257	0.98742349	1.38175280

Table 6.10 shows the effect of the local suction/injection parameter (s) on the local Skin friction, local Nusselt number, and local Sherwood number. It is observed that local Skin friction $f''(0)$, local Nusselt number $-\theta'(0)$ and local Sherwood number $-\phi'(0)$ are increases as the local suction parameter (s) increases.

Table 6.10: Effect of the local suction/injection parameter s on the $f''(0)$, $-\theta'(0)$ and $-\phi'(0)$

s	Time(sec)	$f''(0)$	$-\theta'(0)$	-$\phi'(0)$
1.0	0.6	1.54885777	0.86258012	1.55952883
3	0.3	3.16065571	1.46874149	2.41976386
3.5	0.3	5.07369839	2.21317199	3.47438577

Figure 6.1, the effects of the buoyancy parameter due to temperature λ on the velocity profiles is shown in Fig 6.1. It is seen from this figure that the velocity profiles decrease with an increase of buoyancy parameter λ which demonstrating the usual fact that buoyancy parameter λ stabilizes the boundary layer growth. It is noticed that buoyancy parameter has significant effects on the solutions.

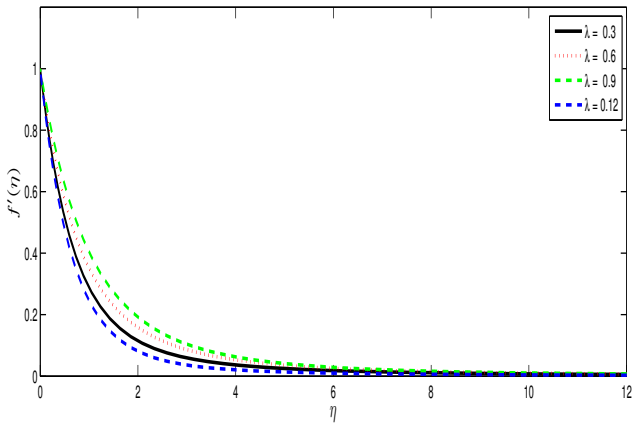

Figure 6.1: Effect of the buoyancy parameter due to temperature (λ) on the velocity profiles

Figure 6.2, shows the effects of magnetic parameter M on the velocity profiles. From different values of magnetic parameter M the velocity profiles is presented in Figure 6.2.

The magnetic parameter (M) is found to retard the velocity at all points. It is because that application of transverse magnetic field will result in a resistive type force which is a Lorentz force similar to drag force which tends to resist the fluid flow and thus dropping its velocity. Thus increasing the magnetic parameter M reduces the boundary layer and thereby reduces the velocity profiles.

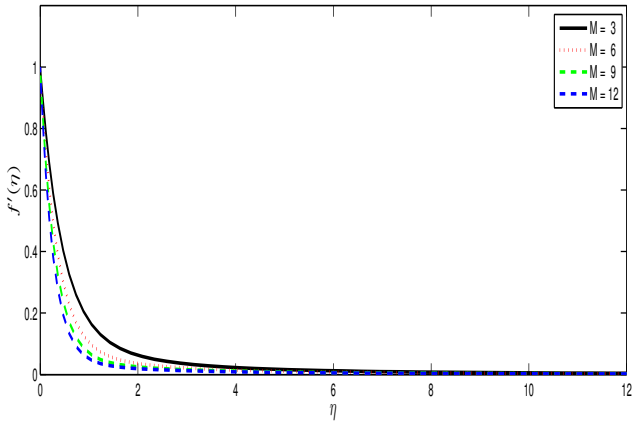

Figure 6.2: Effect of the magnetic parameter (M) on the velocity profiles.

Figures 6.3, 6.4 and 6.5 describe the influence of unsteady parameter (A) on the velocity profile, temperature profile and species concentration, respectively. All these three figures show the dimensionless velocity, dimensionless temperature, and dimensionless species concentration for different values of the unsteady parameter (A). The velocity profiles is presented in Figure 6.3, temperature profiles is presented in Figure 6.4 and concentration is presented in Figure 6.5, respectively. The velocity profiles decreases as unsteady parameter A increases. Increasing the unsteady parameter A effect the velocity boundary surface thickness to decrease. Increasing the value of unsteady parameter A reduces the thermal boundary surface thickness thus reducing the fluid temperature distribution.

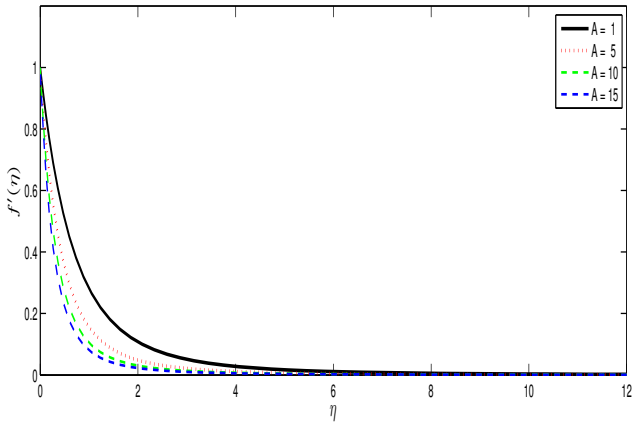

Figure 6.3: Effect of the unsteady parameter (A) on the velocity profiles.

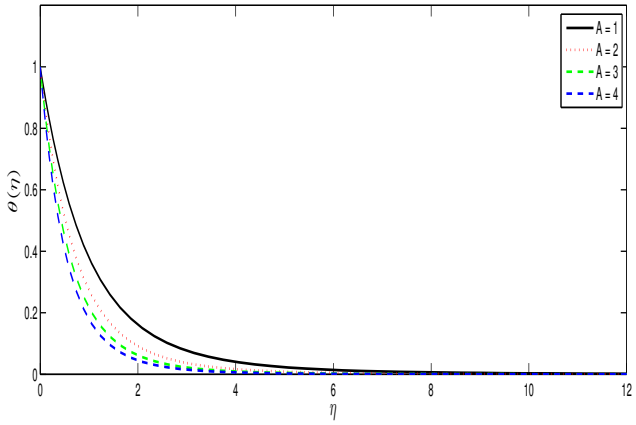

Figure 6.4: Effect of the unsteady parameter (A) on the temperature profiles.

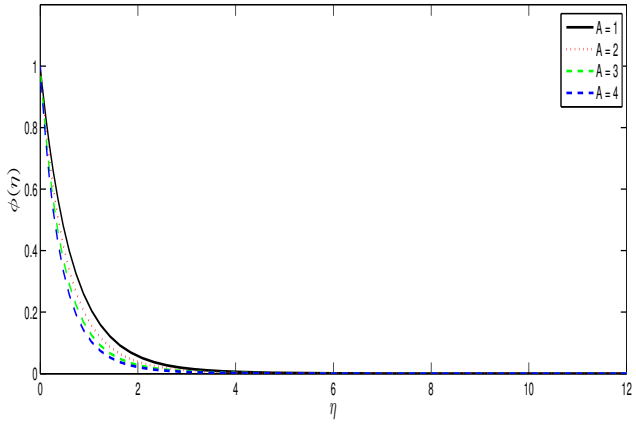

Figure 6.5: Effect of the unsteady parameter (A) on the species concentration.

Figure 6.6, shows the influence of Prandtl number (Pr) on the temperature profile. For the different values of the Prandtl number Pr, the temperature profiles are plotted in Figure 6.6. The Prandtl number defines the ratio of momentum diffusivity to thermal diffusivity. From Fig 6.6, it is observed that an increase in the Prandtl number decreases temperature profiles.

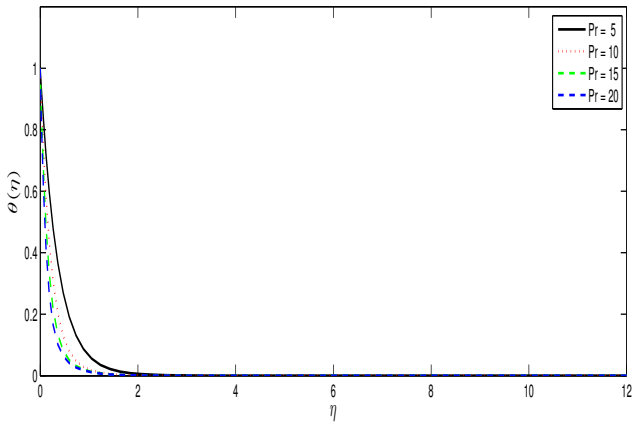

Figure 6.6: Effect of the Prandlt number (Pr) on the temperature profiles.

Figure 6.7, shows the dimensionless temperature profiles inside the boundary layer for different values of the local heat source parameter Q. It is observed that the temperature in the boundary layer increases with increasing values of heat source parameter Q. When $Q < 0$ leads to the decreasing of the thermal boundary surface thickness, while this layer enhances significantly with increase in local heat source parameter Q.

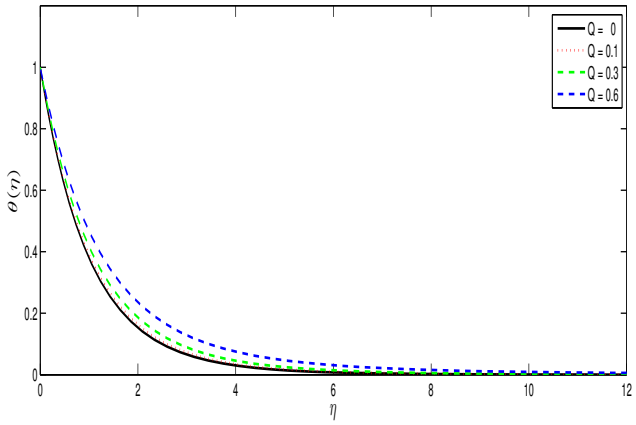

Figure 6.7: Effect of the local heat source parameter (Q) on the temperature profiles.

Figure 6.8, The effect of the radiation parameter (Nr) on the temperature is described by Figure 6.8. The rate of energy transport to the fluid increases by increasing the radiation parameter. Therefore, the temperature of the fluid increases. On the other hand, the increase of radiation parameter leads to overcoming the effect of the convective heat transfer.

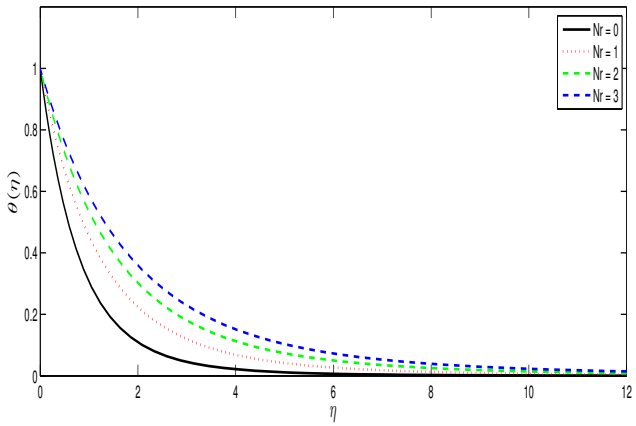

Figure 6.8: Effect of Radiation parameter (Nr) on the temperature profiles.

Figure 6.9, illustrates the concentration profiles for different values of Schmidt number Sc. The Schmidt number Sc represents the ratio of the momentum to the mass diffusivity. The Schmidt number, therefore, quantifies the relative effectiveness of momentum and mass transport by diffusion in the concentration boundary layer. It is observed that as the Schmidt number Sc increases the concentration decreases. The reductions in the concentration profiles are accompanied by simultaneous reductions in the concentration boundary layer.

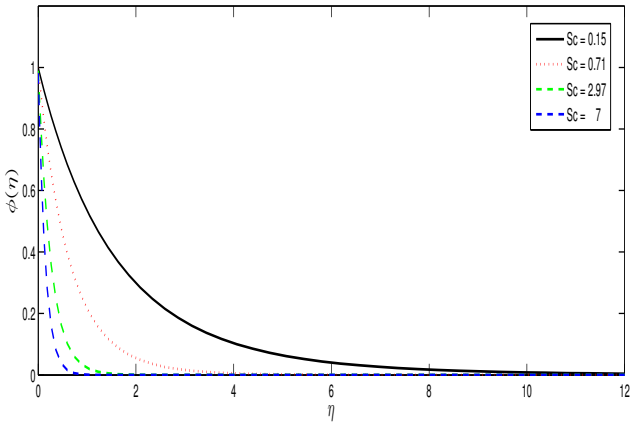

Figure 6.9: Effect of Schmidt number (Sc) on species concentration.

The impact of the chemical reaction (K) on density is shown in Figure 6.10. For different values of the chemical reaction parameter K, the density profiles presented in Figure 6.10. It is obvious that influence of increasing values of chemical reaction K, the concentration distribution across the boundary layer decreases.

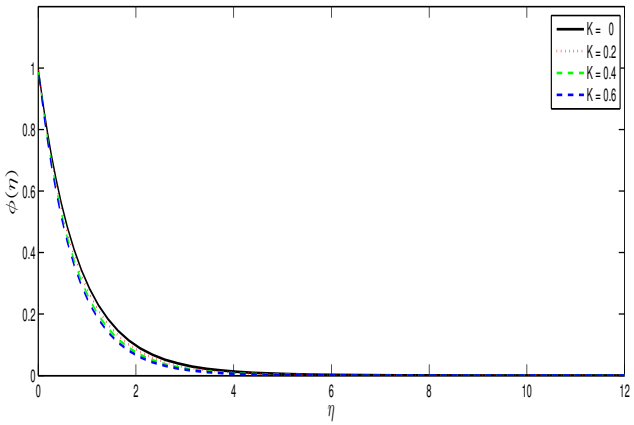

Figure 6.10: Effect of Chemical reaction (K) on species concentration.

Figures 6.11, 6.12 and 6.13 show the effect of local suction parameter (s) on velocity, temperature, and species concentration, respectively. These figures show the dimensionless velocity, dimensionless temperature, and dimensionless species concentration for different values of the local suction/injection parameter (s). The velocity, temperature, and concentration profiles are significantly influenced by the local suction parameter s. On the other hand, eliminating fluid from the fluid flow system through suction, as expected,

significantly reduces the velocity profiles. It is seen that increasing the suction parameter s decreases both temperature and concentration profiles.

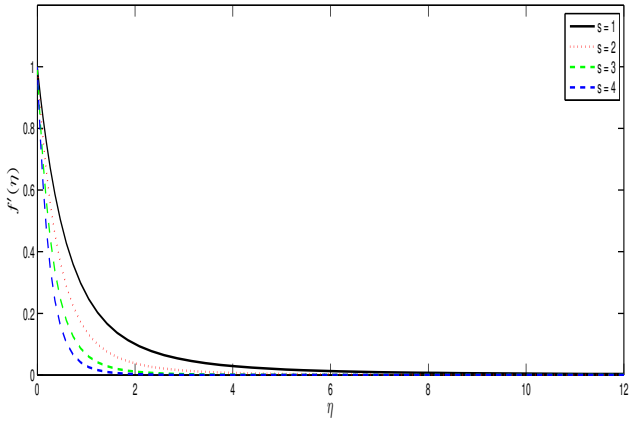

Figure 6.11: Effect of the local suction parameter (s) on the velocity profiles.

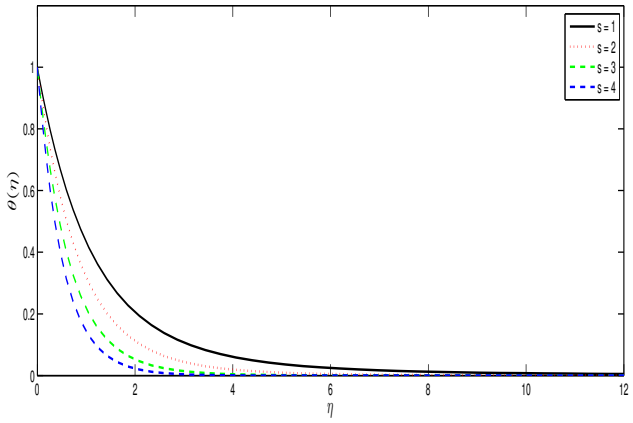

Figure 6.12: Effect of the local suction parameter (s) on the temperature profiles.

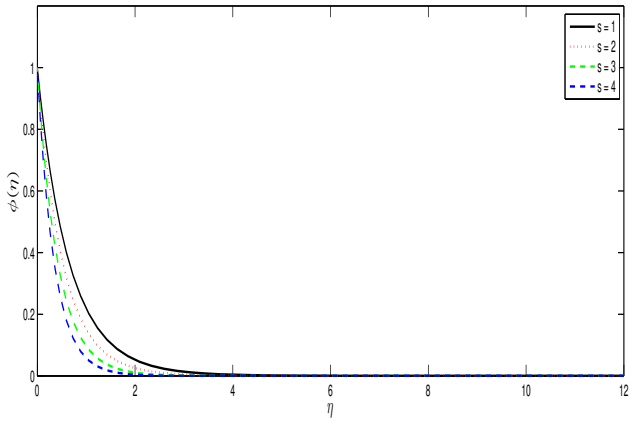

Figure 6.13: Effect of the local suction parameter (s) on the species concentration.

Figures 6.1 to Figure 6.13 represent the velocity, temperature and concentration profiles. The effects of different parameters were observed for velocity, temperature and concentration profiles. We noticed that these parameters have significant effects on velocity, temperature and concentration profiles.

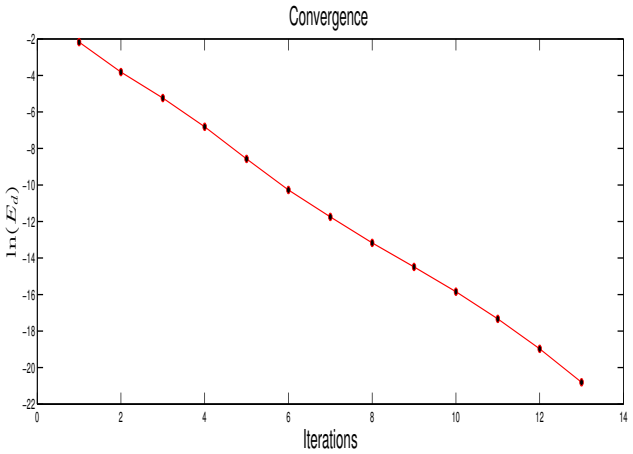

Figure 6.14: Logarithm of SRM decoupling error

The figure shows that the values of the system converge as the iterations increases.

Chapter 7

Conclusion and Recommendations

In this study, we investigated the problem of unsteady hydromagnetic chemically reacting mixed convection MHD fluid flow over a permeable stretching sheet embedded in a porous medium with thermal radiation and heat source. We applied similarity transformation to convert the governing partial differential equations into a system of ordinary differential equations. The transformed ordinary differential equations are then solved numerically by using Spectral Relaxation Method (SRM). The effect of all necessary parameters on dimensionless velocity $f'(\eta)$, temperature $\theta(\eta)$ and species concentration $\phi(\eta)$ have been presented in this study. We found that:

- The velocity profiles decreases as unsteady parameter A increases.
- Increasing the values of the magnetic parameter M decreases velocity of the fluid.
- Enhancement of the Prandlt number Pr decreases temperature.
- The temperature of the fluid decreases as the Unsteady parameter A increases.
- The temperature increases as the local heat source parameter Q increases.
- Increasing the radiation parameter Nr increases temperature.
- Enhancement of the Chemical reaction K decreases species concentration.
- The concentration boundary layer is thicker than temperature boundary layer.
- An increase in the Prandtl number decreases temperature profiles.

Bibliography

[1] Abbasbandy S, Approximate solution for the non-linear model of diffusion and reaction in porous catalysts by means of the homotopy analysis method, Chem. Eng. J., 136(2-3), pp. 144-150, 2008.

[2] Abbasbandy S, The application of homotopy analysis method to non-linear equations arising in heat transfer, Phys. Lett. A, 360, pp. 109-113, 2006.

[3] Alao F.I, Fagbade A.I, and Falodum B.O, Effects of thermal radiation, soret and dufour on an unsteady heat and mass transfer fluid flow of a chemically reacting fluid past a semi-infinite vertical plate viscous dissipation, Journal of the Nigerian Mathematical Society, Vol. 35, pp. 142-158, 2016.

[4] Allan F.M, and Muhammed I.S, On the analytic solution of non-homogeneous Blasius problem, Journal of Computational and Applied Mathematics, Vol. 182, pp. 362-371, 2005.

[5] Allan F.M, Construction of analytic solution to chaotic dynamical systems using the homotopy analysis method, Chaos Soliton. Fract., 39(4), pp. 1744-1752, 2009.

[6] Anderson J.D, Fundamentals of Aerodynamics, 2nd Edition McGraw-Hill, New York, 1991.

[7] Bhattacharyya K, Mukhopadyay S, and Layek G.C, Unsteady MHD boundary layer fluid flow with diffusion and first-order chemical reaction over a permeable stretching sheet with suction or blowing, chemical engineering communications, 2013.

[8] Canuto C, Hussaini M.V, Quarteroni A, and Zang T.A, Spectral methods in fluid dynamics, Springer, verlag, 1958.

[9] Crane L.J, fluid flow past a stretching plate, J. Appl. Math. Phys., 21, pp. 645-647, 1970.

[10] Hayat T, and Javed T, On analytic solution for generalized three-dimensional MHD fluid flow over a porous stretching sheet, Phys. Lett. A, 370, pp. 243-250, 2007.

[11] Ibrahim F.S, Hassanien I.A, and Bakr A.A, Unsteady Magnetohydrodynamic micropolar fluid flow and heat transfer over a vertical porous medium in the presence of thermal and mass diffusion with constant heat source, Can. J. Phys. 82 pp. 775, 2004.

[12] Ibrahim W, and Shanker B, Unsteady MHD mixed convective boundary layer slip flow and heat transfer with thermal radiation and viscous dissipation, Heat Transfer - Asian Res, 43 (5), pp. 412-426, 2014.

[13] Islam, A, Islam, M.M, Rahman, M, Ali, L.E, and Khan, M.S, Unsteady heat transfer of viscous incompressible boundary layer fluid flow through a porous plate with induced magnetic field, Journal of Applied Mathematics and Physics, Vol. 4, pp. 294-306, 2016.

[14] Jha B.K, MHD free convective and mass-transfer flow through a porous medium, Astrophys. Space Sci, pp. 175 -283, 1991.

[15] Khan S, Karim I, and Biswas H.A, Heat generation, thermal radiation and chemical reaction effects on MHD mixed convection flow over an unsteady stretching permeable surface, International Journal of basic and applied science, vol. 01, No. 02, October, 2012.

[16] Mahaboobjam S, Sreelaksmi K, and Sarajamma G, Unsteady MHD mixed convection flow, heat and mass transfer over an exponentially stretching sheet with suction, thermal radiation and hall effect, IOSR Journal of mathematics, vol. 12, pp. 66-77, July, 2016.

[17] Makinde O.D, and Olanrewaju O.P, Unsteady mixed convection with soret and dufour effects past a porours plate moving through a binary mixture of chemically reacting fluid, chemical engineering communications, 198:7, pp. 920-938, 2011.

[18] Makinde O.D, and Tshehla M.S, Unsteady hydromagnetic flow of radiation fluid past a convectively heated vertical plate with the Navier slip, Advances in Mathematical Physics, 17 April, 2014.

[19] Misra M, Ahmand N, and Siddiqui Z.U, Unsteady boundary layer flow past a stretching plate and Heat transfer with variable thermal conductivity, World Journal of Mechanics, 2, pp.35-41, 2012.

[20] Mitiku, D, and Ponnain, D, Unsteady hydromagnetic chemically reacting mixed convection flow over a permeable stretching surface with slip and thermal radiation, Journal of the Nigerian Mathematical society, vol.35, p.p. 245-256, 2016.

[21] Motsa S.S, A new spectral relaxation method for similarity variable non-linear boundary layer flow systems, Chemical Engineering Communications, 201(2), 241-256, 2014.

[22] Motsa S.S, and Makukula Z.G, On spectral relaxation method approach for steady von Kármán flow of a Reiner-Rivlin fluid with Joule heating, viscous dissipation and suction/injection, Central European Journal of Physics, vol. 11, no. 3, pp. 363-374, 2013.

[23] Motsa S. S, A new Spectral relaxation method for similarity variable non-linear boundary layer flow system. July 16, 2013.

[24] @articleCHAMKHA2004217, title = "Unsteady MHD convective heat and mass transfer past a semi-infinite vertical permeable moving plate with heat absorption", journal = "International Journal of Engineering Science", volume = "42", number = "2", pages = "217 - 230", year = "2004", issn = "0020-7225", doi = "https://doi.org/10.1016/S0020-7225(03)00285-4", url ="http://www.sciencedirect.com/science/article/pii/S0020722503002854", author = "Ali J. Chamkha"

[25] Nageeb A.H, Mondal S, and Sibanda P, Unsteady natural convective boundary-layer flow of MHD nanofluid over a stretching surface with chemical reaction using the spectral relaxation method, Procedia Engineering, 18-24, 127, 2015.

[26] Naveed M, Abbas Z, and Sajid M, hydromagnetic flow over an unsteady curved stretching surface, engineering science and technology, an International Journal, 19, pp. 841-845, 2016.

[27] Nayfeh A.H, Introduction to Perturbation Techniques, Wiley, 1979.

[28] Nazar R, Amin N, Filip D, and Pop I, Unsteady boundary layer flow in the region of the stagnation point on a stretching sheet, International Journal of Engineering Science, pp. 1241-1253, 2004.

[29] Patil P.M, Roy S, and Chamkha A.J, Double diffusive mixed convection flow over a moving vertical plate in the presence of internal heat generation and a chemical reaction, Turk J Eng Environ Sci, 33, pp. 193-205, 2009.

[30] Ramachandra P, and Bhaskar R, Radiation and mass transfer effects on an unsteady MHD convective flow past a heated vertical plate in a porous medium with viscous dissipation Theoret Appl Mech, Vol. 34, pp. 135-160, 2007.

[31] Uwanta I.J, and Hamza M.M, Unsteady hydromagnetic flow of a reactive viscous fluid in a vertical channel with thermal diffusion, diffusion-thermal and variable viscosity effects, computational mathematics and modeling, vol.26, No.3, July, 2015.

[32] Rand R.H, and Armbruster D, Perturbation Methods, Bifurcation Theory and Computer Algebraic, Springer, 1987.

[33] Rashidi M.M, Ali M, Rostami B, Rostami P, and Xie G.N, Heat and mass transfer for MHD viscoelastic fluid flow over a vertical stretching sheet with considering soret and dufour effects, Mathematical problems in engineering Hindawi Publishing Corporation, Article ID 861065, 2014.

[34] Seth G.S, Hussain S.M, and Sarkar S, Hydromagnetic natural convection flow with heat and mass transfer of a chemically reacting and heat absorbing fluid past an accelerated moving vertical plate with ramped temperature and ramped surface concentration through a porous medium, Journal of Egyptian Mathematical Society, 23, pp. 197-207, 2015.

[35] Shampine L.F, Kierzenka J, and Reichelt M.V, Solving boundary value problems for ordinary differential equations in MATLAB with bvp4c. October 26, 2000.

[36] Sulochana C, and Kishor M.K, Radiation and chemical reaction effects on MHD thermosolutal nanofluid over a vertical plate in porous medium, Chemical and process engineering research, Vol. 34, 2015.

[37] Trafethen L.N, Spectral methods in matlab, SLAM 2000.

[38] Ullah, I, Bhattacharyya, K, Shafie, S, and Khan, I, Unsteady MHD mixed convection slip flow of Casson fluid over non-linear stretching sheet embedded in a porous medium with chemical reaction, thermal radiation, heat generation/absorption and convection boundary conditions, DOI: 10.137/journal.pone.0165348, 2016.

[39] Vajravelu K, Prasad K.V, and Chiu-On Ng, Unsteady convective boundary layer flow of a viscous fluid at a vertical surface with variable fluid properties, non-linear Analysis: Real World Applications, 14, pp. 455-464, 2013.

[40] Wikipedia dictionary

[41] Williams J.C, and Rhyne T.H, Boundary layer development on a wedge impulsively set into motion, SIAM J. APPl. Math. 38: 215-224 1980.

[42] https://www.thermopedia.com

[43] https://www.thoughtco.com